

Journal of Thermal Analysis and Calorimetry

Thermal analysis of novel biphenylamide derivatives: influence of positional and functional group isomerism on solid state properties

--Manuscript Draft--

Manuscript Number:	JTAC-D-14-01036
Full Title:	Thermal analysis of novel biphenylamide derivatives: influence of positional and functional group isomerism on solid state properties
Article Type:	Original Research
Corresponding Author:	Milan D Antonijevic, Ph.D University of Greenwich Chatham Maritime, Kent UNITED KINGDOM
Corresponding Author Secondary Information:	
Corresponding Author's Institution:	University of Greenwich
Corresponding Author's Secondary Institution:	
First Author:	Samuel K Owusu-Ware, PhD
First Author Secondary Information:	
Order of Authors:	Samuel K Owusu-Ware, PhD Anthony J Cherry, PhD Christine Baltus, PhD John Spencer, PhD Milan D Antonijevic, Ph.D
Order of Authors Secondary Information:	
Abstract:	<p>The physicochemical properties of a small library of 4-methyl-biphenylamide derivatives have been investigated by means of differential scanning calorimetry (DSC), thermogravimetric analysis (TGA) and hot-stage microscopy (HSM). The obtained results show that positional isomerism has a significant influence on the thermal behaviour of the 4-methyl-biphenylamide derivatives. Two polymorphic forms were found for the ortho-substituted derivatives, whilst the para-substituted derivatives exhibit three polymorphic forms. The ortho-substituted biphenylamides were more likely to generate metastable forms when cooled from the melt. Furthermore, self-heating properties were revealed by the para-substituted 4-methyl-biphenylamide derivatives, in which the highly energetic crystallization processes raised the sample temperature by as much as 4°C during cooling. Such a high energy exothermic crystallization process suggests crystallization to be highly favourable, from a thermodynamic standpoint. Hence the p-substituted derivatives are unlikely to generate amorphous forms. Based on the melting points of the most stable polymorphic form (Form I) and the activation energy of the evaporation processes, the para-substituted compounds demonstrate greater thermal stability over their ortho-substituted counterparts. This further suggests that para-substituted compounds, due to their steric effects have greater interactions between individual molecules in the crystalline form.</p>
Suggested Reviewers:	John Murphy, PhD Pfizer Global Research and Development john.murphy3@pfizer.com Dr John Murphy has great expertise in analysing novel polymorphic systems using Thermoanalytical tools.

Thermal analysis of novel biphenylamide derivatives: influence of positional and functional group isomerism on solid state properties

Samuel K Owusu-Ware¹, Anthony J Cherry¹, Christine Baltus¹, John Spencer², Milan D. Antonijevic¹ (✉)

¹Faculty of Engineering and Science, School of Science, University of Greenwich (Medway Campus), Chatham Maritime, Kent ME4 4TB, UK

²Department of Chemistry, School of Life Sciences, University of Sussex, Falmer, BN1 9QJ, UK,

e-mail: M.Antonijevic@greenwich.ac.uk

Key words: Biphenylamide derivatives, polymorphism, stability, crystallisation, differential scanning calorimetry,

ABSTRACT

The physicochemical properties of a small library of 4-methyl-biphenylamide derivatives have been investigated by means of differential scanning calorimetry (DSC), thermogravimetric analysis (TG) and hot-stage microscopy (HSM). The obtained results show that positional isomerism has a significant influence on the thermal behaviour of the 4-methyl-biphenylamide derivatives. Two polymorphic forms were found for the ortho-substituted derivatives, whilst the para-substituted derivatives exhibit three polymorphic forms. The ortho-substituted biphenylamides were more likely to generate metastable forms when cooled from the melt. Furthermore, self-heating properties were revealed by the para-substituted 4-methyl-biphenylamide derivatives, in which the highly energetic crystallization processes raised the sample temperature by as much as 4°C during cooling. Such a high energy exothermic crystallization process suggests crystallization to be highly favourable, from a thermodynamic standpoint. Hence the p-substituted derivatives are unlikely to generate amorphous forms. Based on the melting points of the most stable polymorphic form (Form I) and the activation energy of the evaporation processes, the para-substituted compounds demonstrate greater thermal stability over their ortho-substituted counterparts. This further suggests that para-substituted compounds, due to their steric effects have greater interactions between individual molecules in the crystalline form.

INTRODUCTION

Biphenyls are important structural analogues that have applications across a wide range of industries, from textiles to pharmaceuticals [1-4]. From a pharmaceutical viewpoint, the biaryl scaffold is a “privileged structure”, owing to their ability to provide ligands for multiple receptors [5]. As such, the synthesis of biphenyl derivatives has received a great deal of attention and has resulted in the development of libraries of biphenyl

1 containing compounds that are both important intermediates in the production of pharmaceutically useful active
2 substances, and as potential lead compounds/drug candidates with a wide variety of pharmacological activity.
3
4

5
6 A recent article [6] documents the synthesis and characterization of a biphenyl amide library with interesting
7 solid-state properties, in which the asymmetric unit (*Z*) ranges from 1 to 6. This biphenyl library (consisting of
8 amide functionality of different molecular size and at varying positions on the biaryl scaffold) is therefore an
9 interesting set of compounds to investigate by means of thermal analysis from an academic and industrial
10 perspective. The purpose of this study is to use this library of model compounds to investigate the influence of
11 positional isomerism and the size of the amide substituents on the thermal behaviour of these biphenyl
12 compounds.
13
14
15
16
17
18
19
20
21

22 **MATERIALS AND METHODS**

23 **Materials**

24 N-(4'-Methylbiphenyl-3-yl)acetamide (4-MBA (1)), N-(4'-Methylbiphenyl-3-yl)cyclopropanecarboxamide (4-
25 MBA (2)), N-(4'-Methylbiphenyl-4-yl)acetamide (4-MBA (3)), N-(4'-Methylbiphenyl-4-yl)benzamide (4-MBA
26 (4)) and N-(4'-Methylbiphenyl-4-yl)cyclopropanecarboxamide (4-MBA (5)) were synthesised and crystallised as
27 reported previously (Baltus et al., 2012); the molecular structures are presented in Table 1. All compounds were
28 >95% pure, as determined by ¹H NMR and CHN analysis.
29
30
31
32
33
34
35
36

37 **Table 1 here**
38
39
40
41
42
43
44
45
46
47
48
49
50
51
52
53
54
55
56
57
58
59
60
61
62
63
64
65

1
2 **Instrumentation**

3 Thermogravimetric analysis (TG)

4
5 Modulated thermogravimetric (MTG) and conventional TG studies were performed using Q5000 IR (TA
6 Instruments, UK). All experiments were performed using sample masses of 1.85 ± 0.25 mg in a standard
7 aluminium pan under a nitrogen atmosphere at a flow rate of $25 \text{ cm}^3 \text{ min}^{-1}$. For the TG experiments, samples
8 were heated from ambient temperature to 400°C at 10°Cmin^{-1} . In the MTG studies each sample was equilibrated
9 at 100°C (with the exception of (4-MBA 5, which was equilibrated at 50°C) and heated to 350°C . The
10 temperature modulation settings were $\pm 5^\circ\text{C}$ amplitude for a period of 200 s with an underlying heating rate of
11 5°Cmin^{-1} .
12
13
14
15
16
17
18
19
20
21

22 Differential scanning calorimetry (DSC)

23
24 DSC studies were performed using a Q2000 (TA Instruments, UK) calorimeter under a nitrogen atmosphere at a
25 flow rate of $50 \text{ cm}^3 \text{ min}^{-1}$ in hermetically sealed Tzero aluminium pans. Sample masses of 1.65 ± 0.51 mg were
26 analysed, typically in the temperature range 0 to 250°C using various heating and cooling rates (defined in the
27 accompanying Figures and text).
28
29
30
31
32
33

34 Hot-Stage Microscopy (HSM)

35
36
37 HSM investigations were conducted using an FP8HT hot-stage with an FP90 digital temperature controller
38 (Mettler Toledo, UK) on a DME Model 13595 microscope (Leica Microsystems, China) equipped with a PL-
39 A622 firewire camera (PixiLINK, Canada). Samples were heated from ambient temperature to 250°C at
40 10°Cmin^{-1} .
41
42
43
44
45
46
47
48
49
50
51
52
53
54
55
56
57
58
59
60
61
62
63
64
65

1
2
3
4 **RESULTS**

5
6 The results obtained from TG experiments are presented in Fig.1. All samples, with the exception of 4-MBA
7
8 (5), undergo a single process resulting in 100 % mass loss. Sample 4-MBA (5) undergoes a small change
9
10 between 150 and 200°C with an associated mass loss of $2.5 \pm 0.3\%$ (Table 2) followed by complete loss of
11
12 mass. With the aid of hot-stage microscopy (HSM) all processes observed were found to result from the
13
14 evaporation of the melted samples.

15
16
17 **Fig 1 here**

18
19
20 **Table 2 here**

21
22 MTG experiments were performed to determine the activation energies associated with the evaporation
23
24 processes, to better understand the relative stability differences imposed by the amide substituent positioning
25
26 and the size on the biaryl scaffold. In MTG the linear heating rate is modulated resulting in an oscillating
27
28 temperature programme. The result obtained in this experimental approach enables a model-free determination
29
30 of the activation energy. A theoretical consideration of MTG and the method used to extract kinetic parameters
31
32 are provided elsewhere [7, 8].

33
34 The resultant TG and DTG curves from the MTG experiments are presented in Fig. 2. The two o-substituted
35
36 biphenylamide derivatives (4-MBA (1) and 4-MBA (2)) undergo similar transformations to those observed in
37
38 the conventional TGA experiments, which shows that the evaporation behaviour of these two compounds are
39
40 not influenced by the temperature modulation. However, compounds 4-MBA (3) and 4-MBA (5), which are the
41
42 p-substituted counterparts of compounds 4-MBA (1) and 4-MBA (2) respectively, were significantly influenced
43
44 by the oscillating temperature programme. 4-MBA (3) undergoes two mass loss processes as opposed to the
45
46 single process observed in the conventional TGA. The first of the two mass loss processes observed for 4-MBA
47
48 (5) in the conventional TGA now has a greater percentage loss of mass ($6.0 \pm 0.5\%$) and occurs at a lower
49
50 temperature (100-150°C) in the MTG results.

51
52
53 The first mass loss processes for the p-substituted biphenylamides were confirmed (by HSM) to be melt-
54
55 evaporations of a small cluster of particles that exist in an alternative crystalline form. After evaporation, the
56
57 remaining samples of 4-MBA (4) undergo decomposition (this was confirmed by the presence of a small patch
58
59 of dark residue after the completion of the experiment). It appears that the o- and p-substituted biphenylamide
60
61
62
63
64
65

1 derivatives respond differently to heating rate fluctuation. The p-substituted compounds undergo two
2 evaporation processes, whilst the o-substituted compounds undergo a single process. While positional
3 isomerism influences the TG profile, no differences are observed when the size of the amide substituent is
4 considered.
5
6

7
8 **Fig 2 here**
9

10 An approach employed to investigate the nature of a given reaction in kinetic studies is to monitor how the
11 activation energy value changes as a function of conversion [9-11]; conversion is the fraction of sample that has
12 undergone some chemical or physical transformation. In the case of TG the conversion is related to the mass
13 fraction remaining after a particular process, i.e. the amount of sample remaining. A plot of the activation
14 energy as a function of mass fraction is presented in Fig. 3. In MTG experiments several modulation cycles are
15 needed before a reliable activation energy value is acquired, hence at the beginning of any MTG activation
16 energy plot, unrealistically high data points are observed. The kinetic parameters again become unrealistically
17 high at the end of the experiment, which is due to the absence of any reacting material. Because the values at the
18 two extremes of the data are unreliable, the apparent activation energies associated with the first evaporation
19 process for 4-MBA (3) and 4-MBA (5) and the decomposition process for 4-MBA (4) are ignored. The average
20 activation energies across the mass fraction of 20 to 95 % were calculated and are presented in Table 3.
21
22
23
24
25
26
27
28
29
30
31
32

33 All five samples demonstrated some degree of activation energy dependence on the progression of the
34 evaporation process. As such they all exhibit complex behaviour and are therefore unlikely to follow first order
35 kinetics [12].
36
37
38
39
40

41 **Fig 3 here**
42
43
44

45 **Table 3 here**
46
47
48

49 DSC was employed to investigate the thermotropic transitions of the 4-methyl biphenylamide derivatives. The
50 initial scan shows that all samples, with the exception of 4-MBA (5), exhibit no transitions prior to melting (Fig.
51 4). 4-MBA (5) undergoes several processes before the main melting transition at $213 \pm 1^\circ\text{C}$ (melting of Form I),
52 indicating a mixture of polymorphic forms. When heated from 20°C at a rate of 10°Cmin^{-1} some particles melt
53 at $98 \pm 1^\circ\text{C}$ (Form III), which evaporates immediately (not observed in DSC plot due to hermetic sealing). At
54 $193 \pm 1^\circ\text{C}$ other particles (Form II) melt and crystallize almost immediately at $194 \pm 1^\circ\text{C}$ into needle shaped
55
56
57
58
59
60
61
62
63
64
65

1
2 crystals (Form I). The newly crystallized (Form I) particles and other Form I particles already in the sample then
3 melt at $213 \pm 1^\circ\text{C}$. These inferences are supported by HSM investigations (Fig. 5).

4
5 When a comparison of the melting onset temperatures of the highest melting forms (Form I) detected so far is
6 made between o- and p-substitutions, it becomes clear that positional isomerism has an influence on the physical
7 stability of the biphenyl amides. The onset temperatures of the Form I observed for the p-substituted biphenyl
8 amides are higher than their o-substituted counterparts. For example, Form I of the p-substituted 4-methyl
9 biphenylacetamide (4-MBA (3)) melting onset is at $223 \pm 1^\circ\text{C}$, whilst Form I of the o-substituted 4-methyl
10 biphenylacetamide (4-MBA (1)) has a melting onset at $149 \pm 1^\circ\text{C}$. At the same token, the onset of the highest
11 melting form (Form I) of the p-substituted 4-methyl biphenylcyclopropanecarboxamide (4-MBA (5)) is
12 $208 \pm 1^\circ\text{C}$, which is 13°C higher than that observed for Form I of its o-substituted counterpart (4-MBA (2)),
13 which melts at $195 \pm 1^\circ\text{C}$.

14
15 The DSC results show that molecular size has no influence on the physical stability of these materials. With that
16 said, the compound that exhibits the greatest physical stability is the 4-methyl biphenylbenzamide (4-MBA (4)),
17 which has the largest molecular size of the series of compounds analysed. The onset temperature for the melting
18 transition observed for this compound is $227 \pm 1^\circ\text{C}$.

19
20
21
22
23
24
25
26
27
28
29
30
31
32
33
34
35
36
37
38
39
40
41
42
43
44
45
46
47
48
49
50
51
52
53
54
55
56
57
58
59
60
61
62
63
64
65

Fig 4 here

Fig 5 here

Several temperature programmes, namely different heating and cooling rates, were employed to further investigate the thermotropic behaviour of these 4-methylbiphenylamide derivatives. Compound 4-MBA (4) demonstrated no thermotropic polymorphic behaviour when different heating and cooling rates were employed and is thus ignored.

Ortho-substituted Biphenyl Acetamide (4-MBA (1))

Influence of heating rates

After initially heating past the melting point of Form I, 4-MBA (1) crystallizes into a lower melting form (Form II) upon cooling at 10°Cmin^{-1} . During the second heating cycle (Fig. 6(a)) at 10°Cmin^{-1} , Form II melts at $136 \pm 1^\circ\text{C}$ and crystallizes at $141 \pm 2^\circ\text{C}$ into Form I, which then melts at $149 \pm 1^\circ\text{C}$ (Fig. 6(b)). Increasing the heating

1
2 rate to $50^{\circ}\text{Cmin}^{-1}$ suppresses the crystallization into Form I after Form II melts, hence the reduction in the
3 enthalpy change (ΔH) of Form I from $114 \pm 5 \text{ Jg}^{-1}$ observed at $10^{\circ}\text{Cmin}^{-1}$ to $6 \pm 1 \text{ Jg}^{-1}$ when heated at
4 $50^{\circ}\text{Cmin}^{-1}$. Crystallization of Form I is totally prevented at heating rates above $50^{\circ}\text{Cmin}^{-1}$ (Fig. 6(a)).
5
6

7 **Fig 6 here**

8
9 The heating rate dependence of the melt-crystallization into Form I was investigated further by the application
10 of various heating rates below $50^{\circ}\text{Cmin}^{-1}$ (Fig. 7 (a)) using a constant cooling rate of $10^{\circ}\text{Cmin}^{-1}$. At a very low
11 heating rate ($1^{\circ}\text{Cmin}^{-1}$) it appears that only the melting process of Form I occurs. However with increasing
12 temperature Form II becomes more prominent, as observed by the increase in the signal of the melting
13 endotherm at $136 \pm 1^{\circ}\text{C}$. On closer inspection of the DSC curve obtained at a heating rate of $1^{\circ}\text{Cmin}^{-1}$ (Fig. 7
14 (b)), a broad exothermic solid-solid transition between 100 and 125°C and a small endothermic transition at
15 136°C (melting of Form II) is detected. This is not observed at higher heating rates. This result suggests that
16 when a low heating rate is applied, Form II undergoes a solid-solid transition into Form I. The solid-solid
17 conversion of Form II into Form I is kinetically hindered at higher heating rates; as such the solid-solid
18 conversion occurs at a higher temperature, where it overlaps with the melting process of Form II. It is therefore
19 likely that the crystallization into Form I after Form II melts results from seeding of small amounts of Form I,
20 which is generated by partial conversion of Form II prior to melting. Since the transformation of Form II to
21 Form I is an exothermic process, the thermodynamic relationship between Form II and Form I is monotropic,
22 according to the heat-of-transition rule [13, 14]. This monotropic relationship was confirmed by heating the
23 sample at a scan rate of $1^{\circ}\text{Cmin}^{-1}$ to 130°C , cooling to 0°C and re-heating. On the second heating the solid-solid
24 transition is not observed, only the melting of Form I.
25
26

27 The percentage contribution of the melting enthalpies observed for Form II and Form I to the total enthalpy
28 change observed for both melting endotherms was calculated and plotted as a function of heating rate (Fig. 7
29 (c)). From the graph it is evident 100% of Form I can be generated by heating to 130°C at a heating rates of
30 $\leq 1^{\circ}\text{Cmin}^{-1}$.
31
32
33
34
35
36
37
38
39
40
41

42 **Fig 7 here**

43 Influence of cooling rates

44 Application of different cooling rates appears to have the opposite effect on the ratio of Form II to Form I
45 generated (when compared to that observed when different heating rates are used). At low cooling rates a
46
47
48
49
50
51
52
53
54
55
56
57
58
59
60
61
62
63
64
65

1 greater proportion of Form II is generated upon heating at $10^{\circ}\text{Cmin}^{-1}$, whilst at higher cooling rates a greater
2 proportion of Form I is detected (Fig. 8 (a)).
3

4 At a cooling rate of $1^{\circ}\text{Cmin}^{-1}$ Form II is generated, which on heating melts and undergoes crystallization into
5 Form I. No other transitions are detected below the melting temperature of Form II. When the sample is cooled
6 at $5^{\circ}\text{Cmin}^{-1}$ an exothermic solid-solid transition that overlaps with the melting of Form II is detected (Fig. 8 (b)),
7 as a result a greater ratio of Form I (when compared with that obtained for a cooling rate of $1^{\circ}\text{Cmin}^{-1}$) is
8 observed. This solid state conversion is the transformation of Form II to Form I. As the cooling rate is increased
9 to $\geq 20^{\circ}\text{Cmin}^{-1}$, another exothermic transition (between 40 and 60°C) is detected. These results demonstrate the
10 complex nature of the thermotropic polymorphic behaviour of o-substituted 4-methyl biphenylacetamide (4-
11 MBA (1)).
12
13
14
15
16
17
18
19
20

21 The observation of the exothermic transition between 40 and 60°C (Fig. 8 (b)) can be explained by the HSM
22 results (Fig. 8 (c)). When the sample is allowed to cool (via Newtonian cooling) it exhibits different degrees of
23 super-cooling. As such, the majority of the sample crystallizes into Form II and a certain proportion does not
24 crystallize even when cooled to 0°C . Upon heating, the super-cooled liquid crystallizes into Form II_b (which has
25 a needle like crystal habit) and Form I. The different degrees of super-cooling seem to influence the crystal form
26 that the liquefaction crystallizes into. This rationale is based on the fact that at lower cooling rates a greater
27 proportion of Form II is generated, whilst at higher cooling rates a greater proportion of Form I is generated
28 upon heating. Hence, the increase in the ratio of Form I observed in DSC as the cooling rate is increased is due
29 to the generation of greater amounts of super-cooled liquefactions that are more likely to crystallize into Form I.
30
31
32
33
34
35
36
37
38
39

40 A plot of percentage contribution of the melting enthalpies (heat of fusion) observed for Form II and Form I in
41 this study is presented in Fig. 8 (d). From the graph it is clear that it is not possible to generate 100% Form I or
42 Form II by the cooling rate method.
43
44
45
46

47 **Fig 8 here**

48 **Ortho-substituted Biphenyl cyclopropanecarboxamide (4-MBA (2))**

49
50 Varying the heating rate has no effect on the phase behaviour of 4-MBA (2) i.e. the sample undergoes a single
51 melting process when cooled at $10^{\circ}\text{Cmin}^{-1}$ and heated at various heating rates (Fig 9 (a)). When the sample is
52 heated at $10^{\circ}\text{Cmin}^{-1}$ after being subject to high cooling rates $\geq 100^{\circ}\text{Cmin}^{-1}$, it undergoes a solid-solid transition
53 into Form I which melts at $195 \pm 1^{\circ}\text{C}$. Hence when 4-MBA (2) is cooled very fast it crystallizes into a
54
55
56
57
58
59
60
61
62
63
64
65

1
2
3
4
5
6
7
8
9
10
11
12
13
14
15
16
17
18
19
20
21
22
23
24
25
26
27
28
29
30
31
32
33
34
35
36
37
38
39
40
41
42
43
44
45
46
47
48
49
50
51
52
53
54
55
56
57
58
59
60
61
62
63
64
65

metastable form (Form II), which is not observed at lower cooling rates. The transformation of Form II into Form I (at $52 \pm 1^\circ\text{C}$) is irreversible and the fact that the heat of transition is exothermic confirms the thermodynamic relationship between the two crystal forms to be monotropic.

At 1°Cmin^{-1} cooling rate the exothermic crystallization of 4-MBA (2) is so energetic that it appears to self-heat i.e. the temperature of the sample is raised temporarily before it continues cooling (Fig. 9 (a)); a phenomenon that is not observed for any of the other cooling rates employed or for 4-MBA (1) at the same cooling rate. The exothermic crystallization, upon cooling, raises the temperature of the sample by $\sim 1^\circ\text{C}$.

Fig 9 here

Para-substituted Biphenyl Acetamide (4-MBA (3))

Application of various heating and cooling rates revealed three polymorphic forms of 4-MBA (3). At very high heating rates ($150^\circ\text{Cmin}^{-1}$) 4-MBA (3) exhibits two melting endotherms (Fig. 10 (a)). The lower melting endotherm (Form II) is only detected when the sample is heated $\geq 100^\circ\text{Cmin}^{-1}$ or above and appears as a small shoulder on the melting of Form I, at $224 \pm 1^\circ\text{C}$. This suggests that cooling compound 4-MBA (3) at 10°Cmin^{-1} generates a mixture of solid forms i.e. Form I and small amounts of Form II, which can only be detected at very high heating rates.

When the sample is subjected to different cooling rates and heated at 10°Cmin^{-1} , three processes are detected (Fig. 10 (b)). The first is a melting process with an onset temperature of $203 \pm 1^\circ\text{C}$, which overlaps with a crystallization exotherm at $214 \pm 1^\circ\text{C}$. The crystallization generates a new crystal form which melts $222 \pm 1^\circ\text{C}$. The melting temperature of this new crystal form is 2°C lower than that observed for Form I ($224 \pm 1^\circ\text{C}$) but has a similar melting enthalpy ($141 \pm 5 \text{ Jg}^{-1}$) and is therefore denoted Form I_b. Varying the heating rates has no effect on the processes observed.

The crystallization of the melt upon cooling of 4-MBA (3) also exhibits a highly energetic exothermic process, that results in the self-heating of the sample (Fig. 10 (c)). At a low cooling rate (1°Cmin^{-1}) the sample temperature increases by $3.5^\circ\text{C} \pm 0.5$ during the crystallization process before it continues cooling, whilst at a higher cooling rate $\geq 60^\circ\text{C}$ the increase in temperature is $\leq 1^\circ\text{C}$.

Fig 10 here

Para-substituted Biphenyl cyclopropanecarboxamide (4-MBA (5))

1 As previously explained, the initial 4-MBA (5) sample consists of three crystalline forms. When the sample is
2 heated past the melting point of Form I and cooled, Form III and Form II are not detected upon the second
3 heating. However, at heating rates $\geq 50^{\circ}\text{Cmin}^{-1}$, the melting point of Form II is detected, which crystallizes into
4 Form I before melting again (Fig. 11 (a)).
5
6

7
8 The behaviour of 4-MBA (5) was found to be influenced by varying the cooling rate (Fig. 11 (b)). At a lower
9 cooling rate (1 to $5^{\circ}\text{Cmin}^{-1}$) only the melting endotherm of Form I is detected. However at a cooling rate of
10 $10^{\circ}\text{Cmin}^{-1}$ or more, the sample crystallizes into Form II and Form I. This is supported by HSM (Fig. 11 (c))
11 investigations which show the needle-dendritic morphology of Form I and the irregularly shaped cubic
12 morphology of Form II. Form II melts at $193 \pm 1^{\circ}\text{C}$ and the melt is seeded by Form I crystals in close proximity,
13 generating more Form I crystals which then melts at $213 \pm 1^{\circ}\text{C}$.
14
15
16
17
18
19
20

21 **Fig 11 here**
22

23 **DISCUSSION**

24 The results obtained demonstrate that the molecular size of the amide substituents on the biphenyl scaffold
25 cannot be correlated with any of the thermal properties investigated by means of TG and DSC. However, some
26 interesting relationships were observed when positional isomerism is considered.
27
28
29
30
31

32
33 From the TG investigation it has been highlighted that the p-substituted biphenyl amides undergo two stage
34 evaporation processes. These evaporation processes result from the melting of different crystalline forms of the
35 compounds. However, only a single evaporation process is observed for the o-substituted biphenylamides. A
36 comparison between the DTG peak temperature of the second evaporation process, observed for para-
37 substituted biphenylamides, with that of the o-substituted biphenylamides show para-directing substitutions to
38 improves the thermal stability of these compounds i.e. the o-substituted biphenylacetamide and
39 biphenylcyclopropanecarboxamide have a DTG peak of evaporation at 322 and 341°C , respectively, whilst p-
40 substituted biphenylacetamide and biphenylcyclopropanecarboxamide have DTG peak of evaporation at 331
41 and 347°C , respectively.
42
43
44
45
46
47
48
49
50
51

52
53 Whilst the calculated average activation energies for the samples may be considered similar, there are
54 differences observed that are greater than their standard deviations (Table 2). When the two biphenylacetamides
55 (4-MBA (1) and 4-MBA (3) are compared, it is found that the p-substitutions have higher activation energy of
56
57
58
59
60
61
62
63
64
65

1
2 evaporation ($97 \pm 12 \text{ kJmol}^{-1}$) than that observed for the o-substitution ($75 \pm 7 \text{ kJmol}^{-1}$). Similar behaviour is
3
4 observed for the biphenylcyclopropanecarboxamides i.e. the para-substitutions exhibit higher activation energy
5 ($99 \pm 24 \text{ kJmol}^{-1}$) when compared with the o-substitution ($78 \pm 5 \text{ kJmol}^{-1}$). This indicates that the p-substituted
6 are more kinetically stable, as they exhibit higher activation energy barrier that must be overcome for the
7 evaporation process to progress.
8
9

10
11 The reason for the differences observed in the thermal and kinetic stability between the o- and p-substitutions of
12 these biphenyls is unclear. However it is inferred that such behaviour could be due to the difference in the
13 ability of molecules to interact, which is influenced by attractive/repulsive forces and the spatial arrangements
14 of the molecules in the liquid state.
15
16
17
18
19
20
21

22 When the melting peak temperature of the highest melting forms (Form I) are compared, p-substituted
23 biphenylamides generally exhibit higher thermo-physical stability i.e. the temperature of their Form I crystals
24 are higher than those of o-substituted biphenylamides. This is due to better molecular stacking ability of p-
25 substitution compared to o- substituted compounds. Similar observations could not be made when the
26 enthalpies (Jg^{-1}) of the melts are considered. Hence the energy required to convert Form I, of the biphenylamide
27 derivatives studied, to liquid does not seem to be correlated with positional isomerism or molecular size.
28
29
30
31
32
33
34
35

36 It appears that it is possible to differentiate the polymorphic behaviour of o- from p-substitutions. The o-
37 substituted biphenylamides seem to have the tendency to generate metastable forms upon cooling the neat
38 liquid, that converts to the more stable forms i.e. they undergo solid-solid transitions into the more stable form
39 on heating. The p-substituted biphenylamides, on the other-hand, crystallize into two forms that melt upon
40 heating.
41
42
43
44
45
46
47

48 An aspect of this study was to probe the notion that the Z' value (the number of molecular formula unit within a
49 unit cell) has some influence on the number of possible crystal forms/transformation that can be found. It was
50 therefore of interest to examine the relationship between the number of polymorphic transformations detected
51 and the Z' value. In the previous study, compounds 4-MBA (3) and 4-MBA (5) were found to generate crystals
52 with the highest Z' values (> 1) of the biphenylamide compounds synthesised [6]. This suggest that these two
53 compounds should exhibit greater degree of polymorphism i.e. they can undergo a greater number of crystalline
54
55
56
57
58
59
60
61
62
63
64
65

1 arrangements, when compared with 4-MBA (1), 4-MBA (2) and 4-MBA (4), all of which have Z' values of 1.
2 The results obtained, however, demonstrate that this is not the case when thermotropic polymorphism is of
3 concern. With the exception of 4-MBA (4), which did not exhibit any thermotropic transition/conversions, all
4 compounds exhibit at least two thermotropic phases regardless of the Z' values. However, compound 4-MBA
5 (3) which was found in previous study to exhibit the unusual Z' value of 6 was found to demonstrate highly
6 unusual, highly energetic crystallization process, which causes the sample's temperature to be raised by $>3^{\circ}\text{C}$
7 during cooling. The relatively high energy associated with the crystallization of compound 4-MBA (3) is likely
8 due to the higher number of molecular formula units (6 molecules) condensing and forming hydrogen bonding
9 within a single asymmetric unit cell.
10
11
12
13
14
15
16
17
18
19

20 CONCLUSIONS

21 This investigation has demonstrated that the 4-methyl-biphenyl derivatives studied undergo thermotropic
22 polymorphism, in which at least two crystal forms are detected with the exception of N-(4'-methylbiphenyl-4-
23 yl)benzamide (4-MBA (4)), which melts at $227 \pm 1^{\circ}\text{C}$. N-(4'-methylbiphenyl-3-yl)acetamide (4-MBA (1)) has
24 two thermotropic polymorphic forms, Form II melts at $36 \pm 1^{\circ}\text{C}$, crystallizes at $141 \pm 2^{\circ}\text{C}$ into Form I which
25 melts at $149 \pm 1^{\circ}\text{C}$. N-(4'-Methylbiphenyl-3-yl)cyclopropanecarboxamide (4-MBA (2)) crystallizes into Form II
26 when the melt is cooled at $\geq 100^{\circ}\text{Cmin}^{-1}$. Form II converts at $52 \pm 1^{\circ}\text{C}$ into Form I which melts at $195 \pm 1^{\circ}\text{C}$.
27 Three polymorphic forms were found for N-(4'-Methylbiphenyl-4-yl)acetamide (4-MBA (3)). For this
28 compounds Form II melts at $203 \pm 1^{\circ}\text{C}$, Form I (melts at $224 \pm 1^{\circ}\text{C}$) and Form I_b melts at $222 \pm 1^{\circ}\text{C}$. N-(4'-
29 Methylbiphenyl-4-yl)cyclopropanecarboxamide (4-MBA (5)) also exhibits three polymorphic forms in which
30 Form III melts at $98 \pm 1^{\circ}\text{C}$, Form II at $193 \pm 1^{\circ}\text{C}$ and Form I at $213 \pm 1^{\circ}\text{C}$.
31
32
33
34
35
36
37
38
39
40
41
42
43
44

45 The results presented show that it is possible to correlate certain parameters of thermal properties of materials
46 with positional isomerism. For the 4-methyl-biphenylamide derivatives studied, it was found that the thermo-
47 physical stability is significantly enhanced when the amide substituent is directed in the para- position as
48 opposed to the ortho position of the 4-biphenyl scaffold. For example, the kinetic stability of the evaporation
49 process of these compounds is improved by steering the amide substituents in the para position. Furthermore the
50 ortho-substituted 4-methyl-biphenylamides are more likely to generate metastable forms during crystallization
51 from the melt. On the other hand, p-substitution of the amides on the 4-methyl-biphenyl scaffold generates
52 materials with highly energetic crystallization process that raises the sample temperature during cooling, even at
53
54
55
56
57
58
59
60
61
62
63
64
65

1 a cooling rate of $10^{\circ}\text{Cmin}^{-1}$, a phenomenon that was not observed for the o-substituted amides at the same
2 cooling rate. The material that demonstrates the most energetic crystallization process is N-(4'-methylbiphenyl-
3 4-yl)acetamide (4-MBA (3)). Such high energy exothermic crystallization process suggests crystallization to be
4 highly favourable, from a thermodynamic stand point. Hence the p-substituted 4-methyl-biphenylamide
5 derivatives are unlikely to generate amorphous forms.
6
7
8
9

10
11
12 It was not possible to correlate molecular size with any of the parameters associated with the thermal properties
13 of the biphenyl derivatives studied. Perhaps this is due to the fact that molecular size differences investigated are
14 not great enough to generate any observable differences.
15
16
17
18
19
20
21

22 REFERENCES

- 23
- 24
- 25
- 26 1. Jain ZJ, Gide PS, Kankate RS. Biphenyls and their derivatives as synthetically and pharmacologically
27 important aromatic structural moieties. *Arabian Journal of Chemistry* 2013; (0).
- 28
- 29 2. Wang C, Dong J, Zhang Y, et al. Design, synthesis and biological evaluation of biphenyl urea
30 derivatives as novel VEGFR-2 inhibitors. *MedChemComm* 2013; 4(11): 1434-8.
- 31
- 32 3. Donato L, Mourou A, Davenport CM, et al. Water-Soluble, Donor–Acceptor Biphenyl Derivatives in
33 the 2-(o-Nitrophenyl)propyl Series: Highly Efficient Two-Photon Uncaging of the Neurotransmitter γ -
34 Aminobutyric Acid at $\lambda=800$ nm. *Angewandte Chemie International Edition* 2012; 51(8): 1840-3.
- 35
- 36 4. Chen S, Fahmi NE, Bhattacharya C, et al. Fluorescent Biphenyl Derivatives of Phenylalanine Suitable
37 for Protein Modification. *Biochemistry* 2013; 52(47): 8580-9.
- 38
- 39 5. Costantino L, Barlocco D. Privilege Structures as Leads in Medicinal Chemistry. *Current Medicinal*
40 *Chemistry* 2006; 13(1): 65-85.
- 41
- 42 6. Baltus CB, Press NJ, Antonijevic MD, Tizzard GJ, Coles SJ, Spencer J. Synthesis of a biphenyl library
43 for studies of hydrogen bonding in the solid state. *Tetrahedron* 2012; 68(45): 9272-7.
- 44
- 45 7. Gracia-Fernández CA, Gómez-Barreiro S, Ruíz-Salvador S, Blaine R. Study of the degradation of a
46 thermoset system using TGA and modulated TGA. *Progress in Organic Coatings* 2005; 54(4): 332-6.
- 47
- 48 8. Cheng K, Winter WT, Stipanovic AJ. A modulated-TGA approach to the kinetics of lignocellulosic
49 biomass pyrolysis/combustion. *Polymer Degradation and Stability* 2012; 97(9): 1606-15.
- 50
- 51 9. Brown ME, Maciejewski M, Vyazovkin S, et al. Computational aspects of kinetic analysis: Part A: The
52 ICTAC kinetics project-data, methods and results. *Thermochimica Acta* 2000; 355(1-2): 125-43.
- 53
- 54 10. Keuleers RR, Janssens JF, Desseyn HO. Comparison of some methods for activation energy
55 determination of thermal decomposition reactions by thermogravimetry. *Thermochimica Acta* 2002;
56 385(1-2): 127-42.
- 57
- 58 11. Khawam A, Flanagan DR. Basics and applications of solid-state kinetics: A pharmaceutical
59 perspective. *Journal of Pharmaceutical Sciences* 2006; 95(3): 472-98.
60
61
62
63
64
65

12. Owusu-Ware SK, Chowdhry BZ, Leharne SA, Antonijević MD. Quantitative analysis of overlapping processes in the non-isothermal decomposition of chlorogenic acid by peak fitting. *Thermochimica Acta* 2013; 565(0): 27-33.
13. Burger A, Ramberger R. On the polymorphism of pharmaceuticals and other molecular crystals. I. *Microchimica Acta* 1979; 72(3): 259-71.
14. Burger A, Ramberger R. On the polymorphism of pharmaceuticals and other molecular crystals. II. *Microchimica Acta* 1979; 72(3): 273-316.

1
2
3
4
5
6
7
8
9
10
11
12
13
14
15
16
17
18
19
20
21
22
23
24
25
26
27
28
29
30
31
32
33
34
35
36
37
38
39
40
41
42
43
44
45
46
47
48
49
50
51
52
53
54
55
56
57
58
59
60
61
62
63
64
65

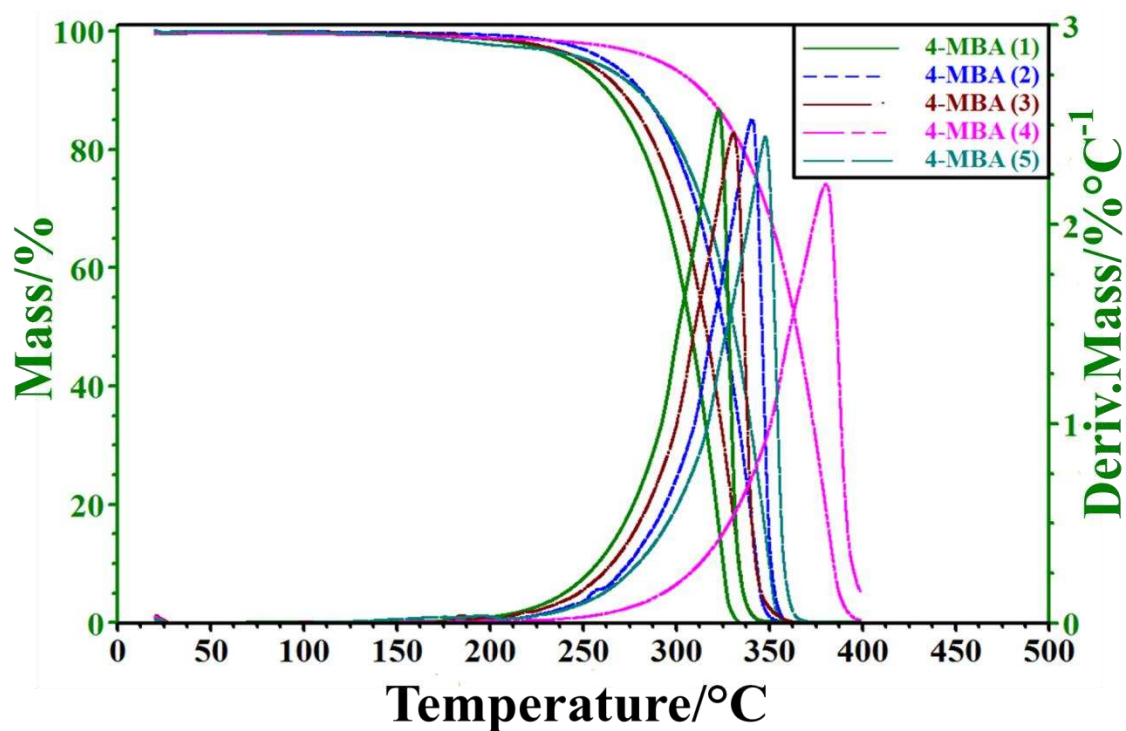


Fig. 1. TG and DTG curves obtained for the 4-methyl-biphenylamide derivatives in a standard TG experiments. Samples were heated from ambient temperature to 400°C at 10°Cmin⁻¹.

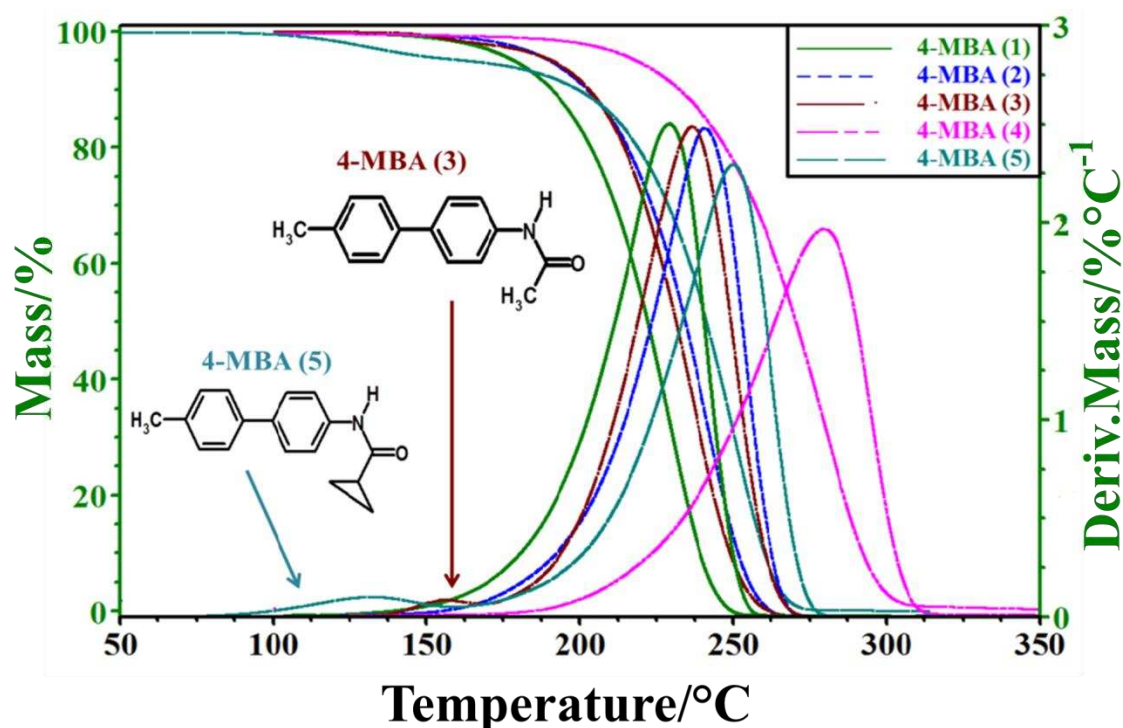


Fig. 2. TG and DTG curves obtained for the 4-methyl-biphenylamide derivatives in modulated TG experiment. Samples were heated from 100°C (with the exception of 4-MBA 5, which was equilibrated at 50°C) to 350°C at a modulation settings of +/-5°C amplitude for a period of 200 s with an underlying heating rate of 5°Cmin⁻¹.

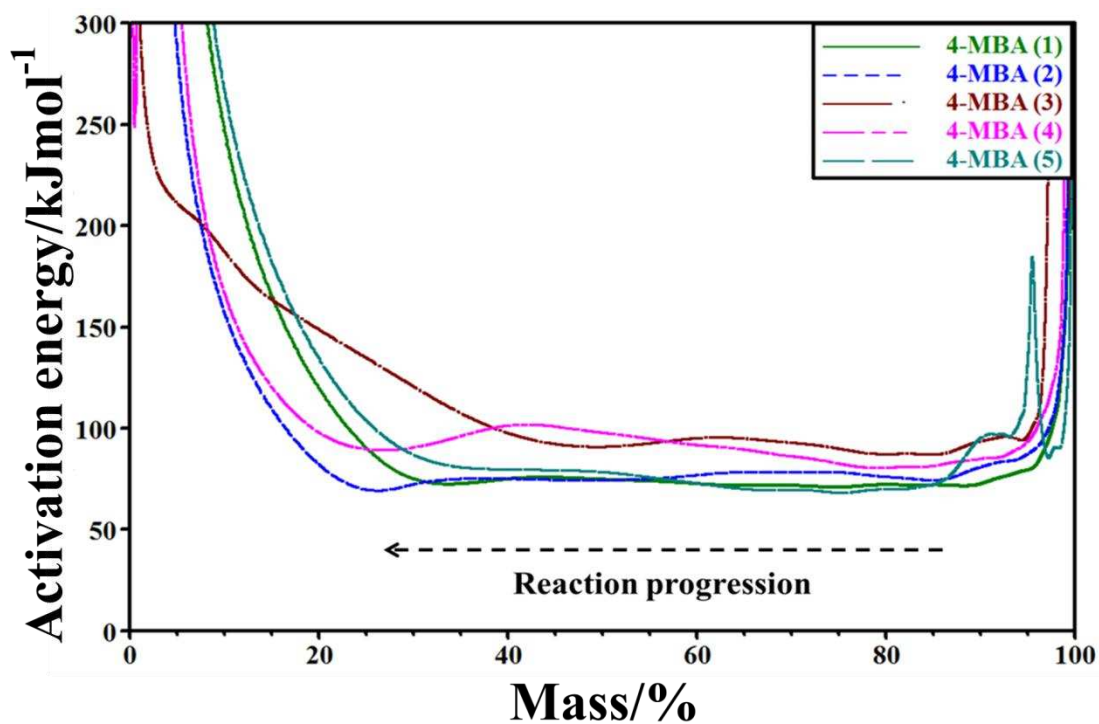


Fig. 3. Activation energies obtained from MTG experiments as a function of change in mass of the 4-methyl-biphenylamide derivatives.

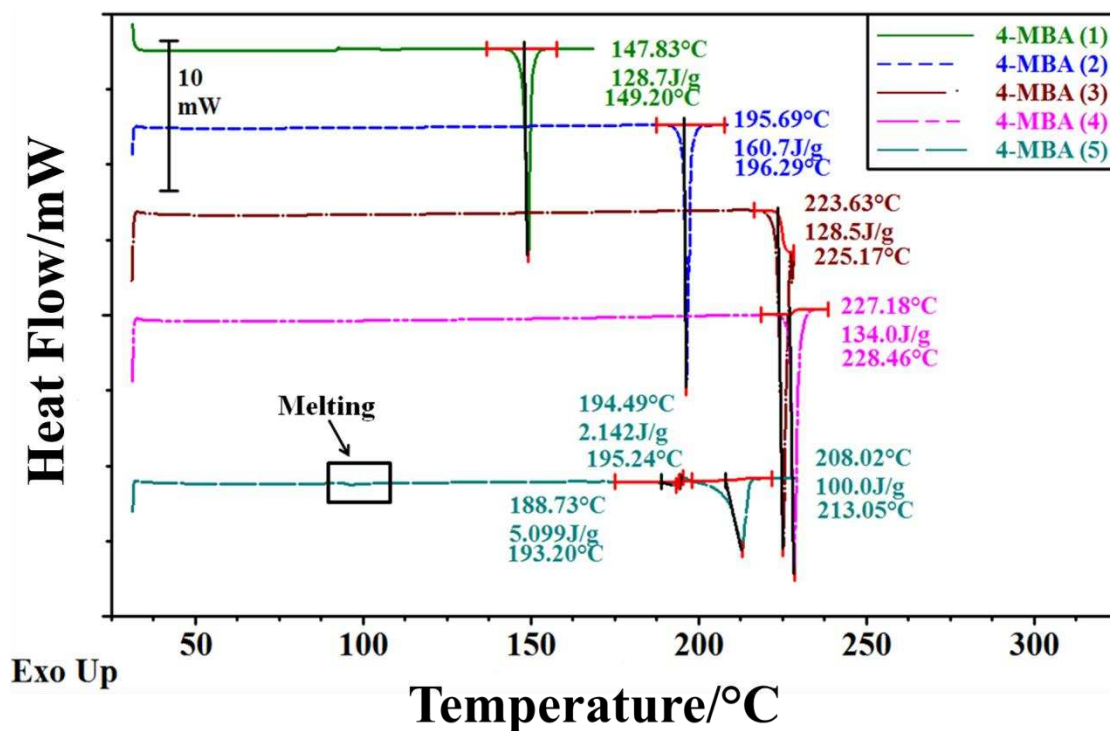


Fig. 4. DSC curve overlay of the initial heating of the 4-methyl-biphenylamide derivatives obtained at a heating rate of $10^{\circ}\text{Cmin}^{-1}$.

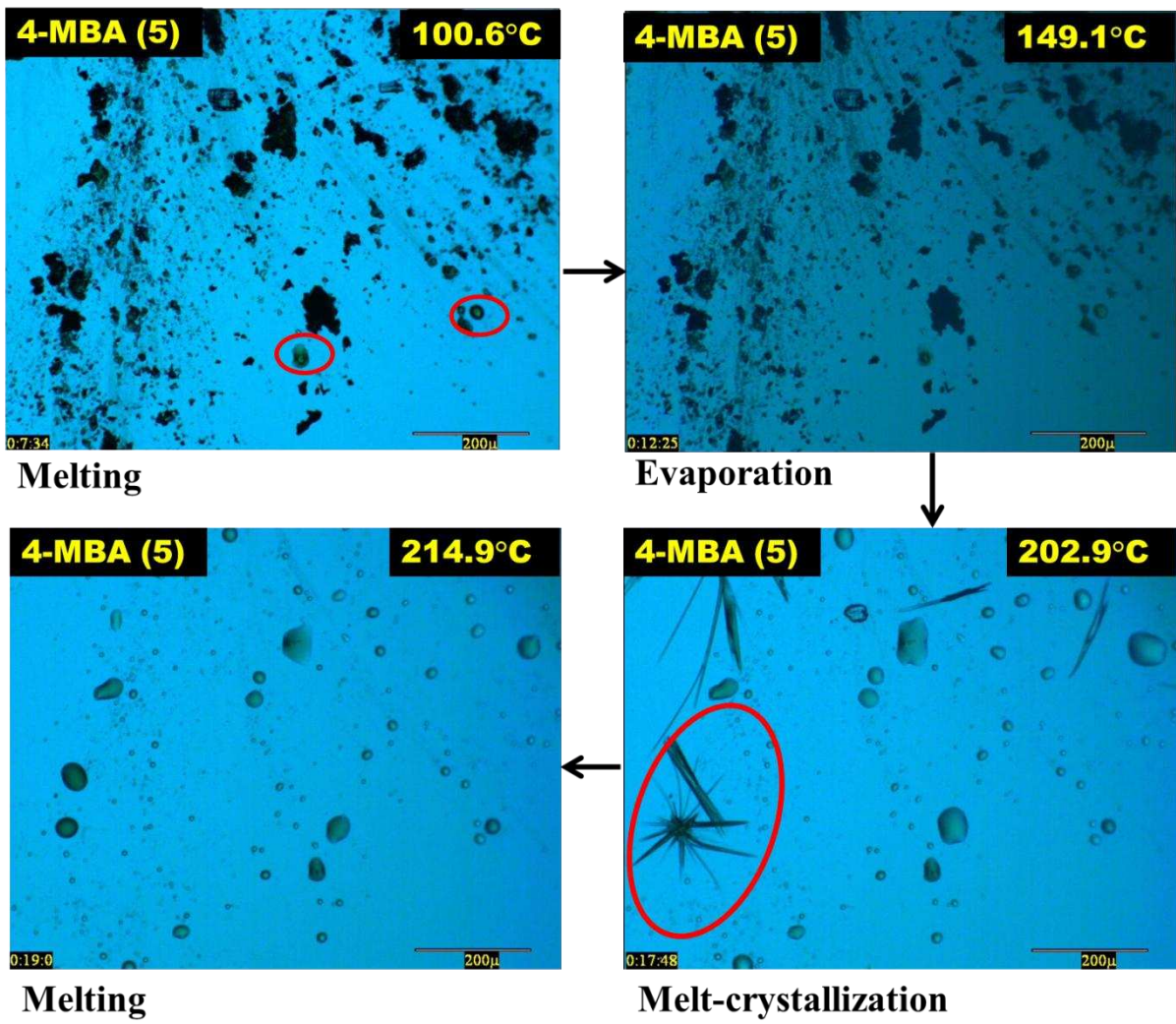


Fig. 5. HSM images of 4-MBA (5) heated from 25°C to 250°C at 10°Cmin⁻¹.

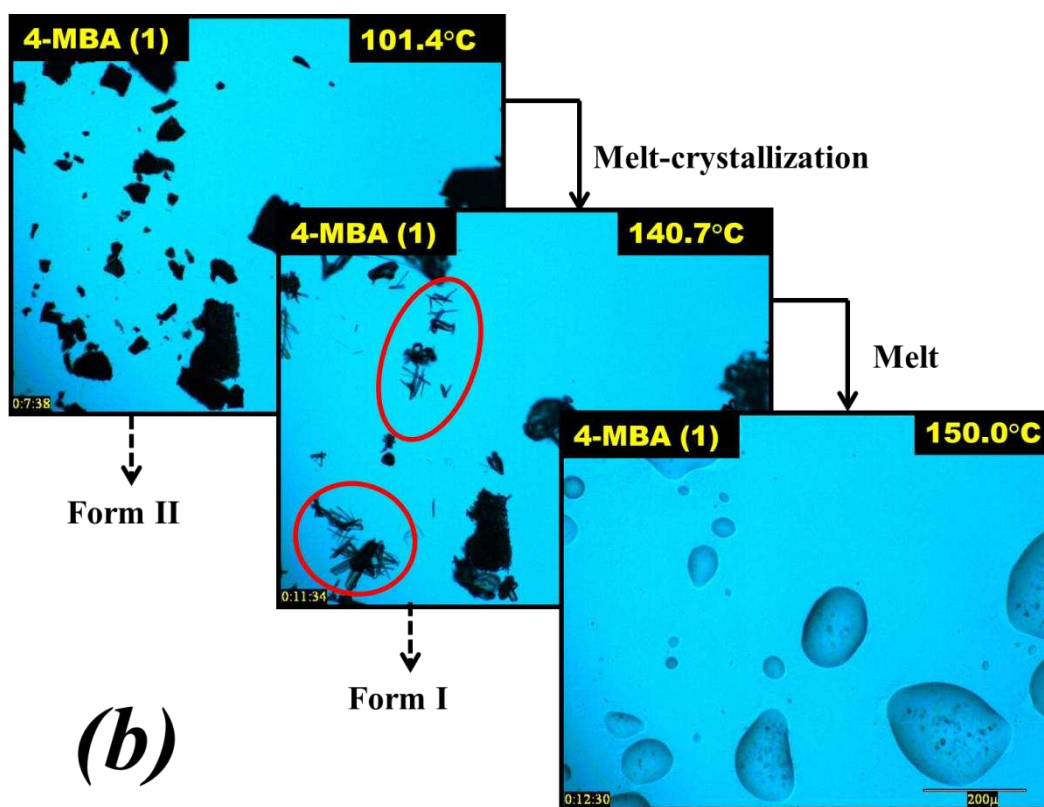
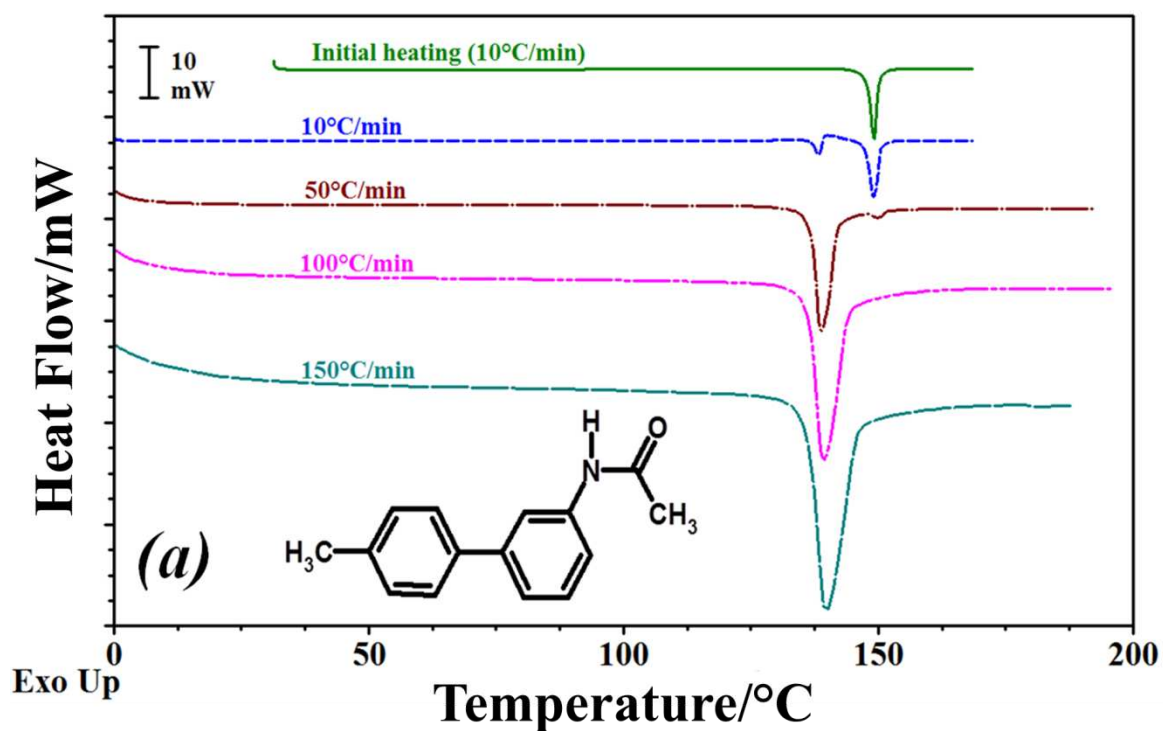
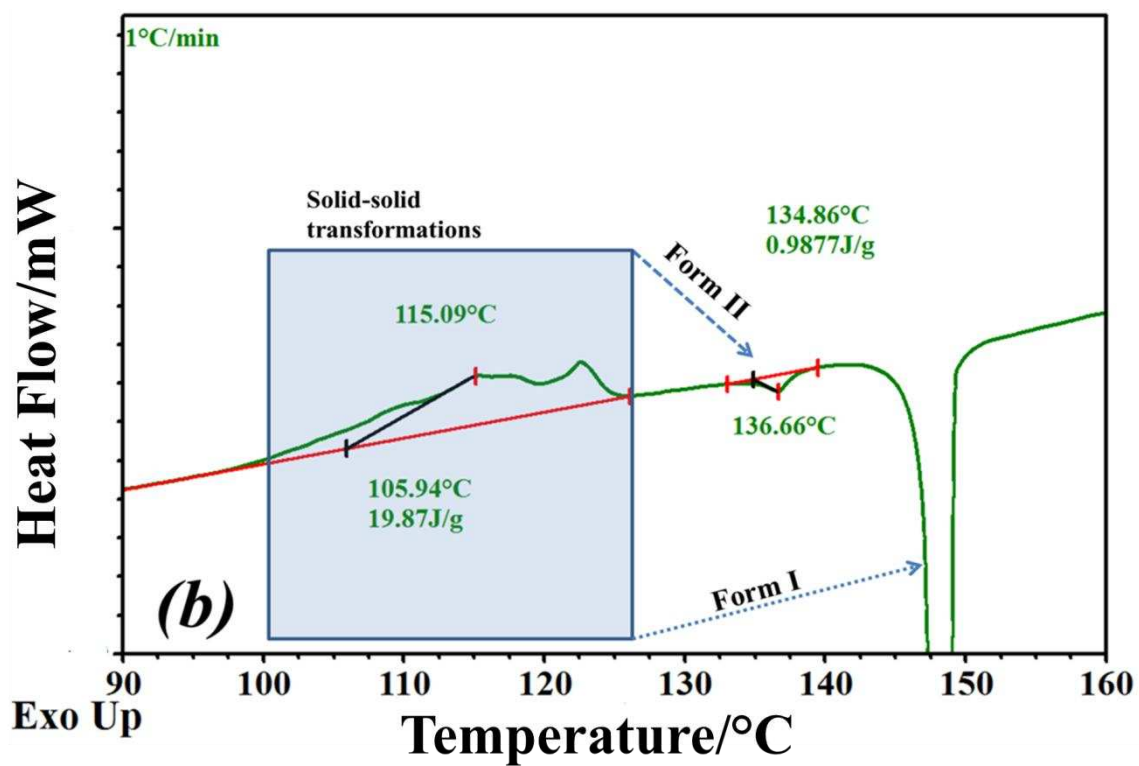
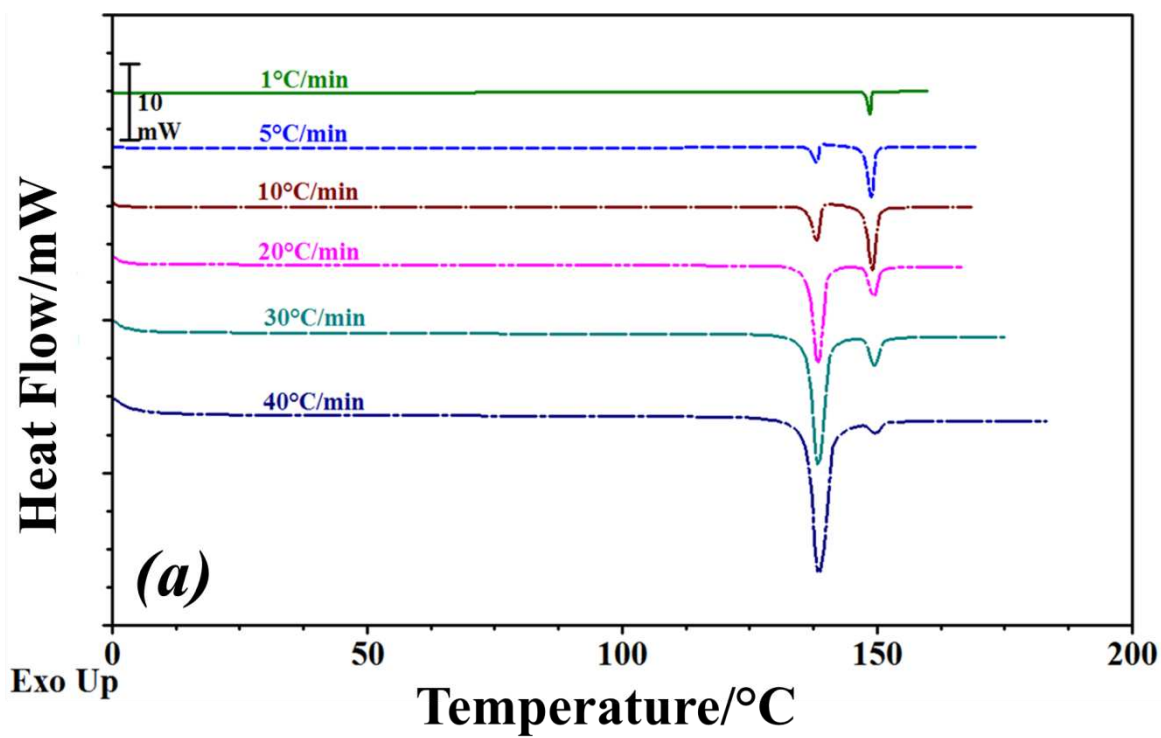


Fig. 6 (a) DSC curve overlay of 4-MBA (1) heated at various heating rates after cooling at a rate of $10^{\circ}\text{Cmin}^{-1}$ and (b) HSM images of key transitions observed for 4-MBA (1) when heated at $10^{\circ}\text{Cmin}^{-1}$ between 25 and 170°C . Starting material (Form II) was prepared by melting the initial sample and cooling over liquid nitrogen before being examined by HSM.



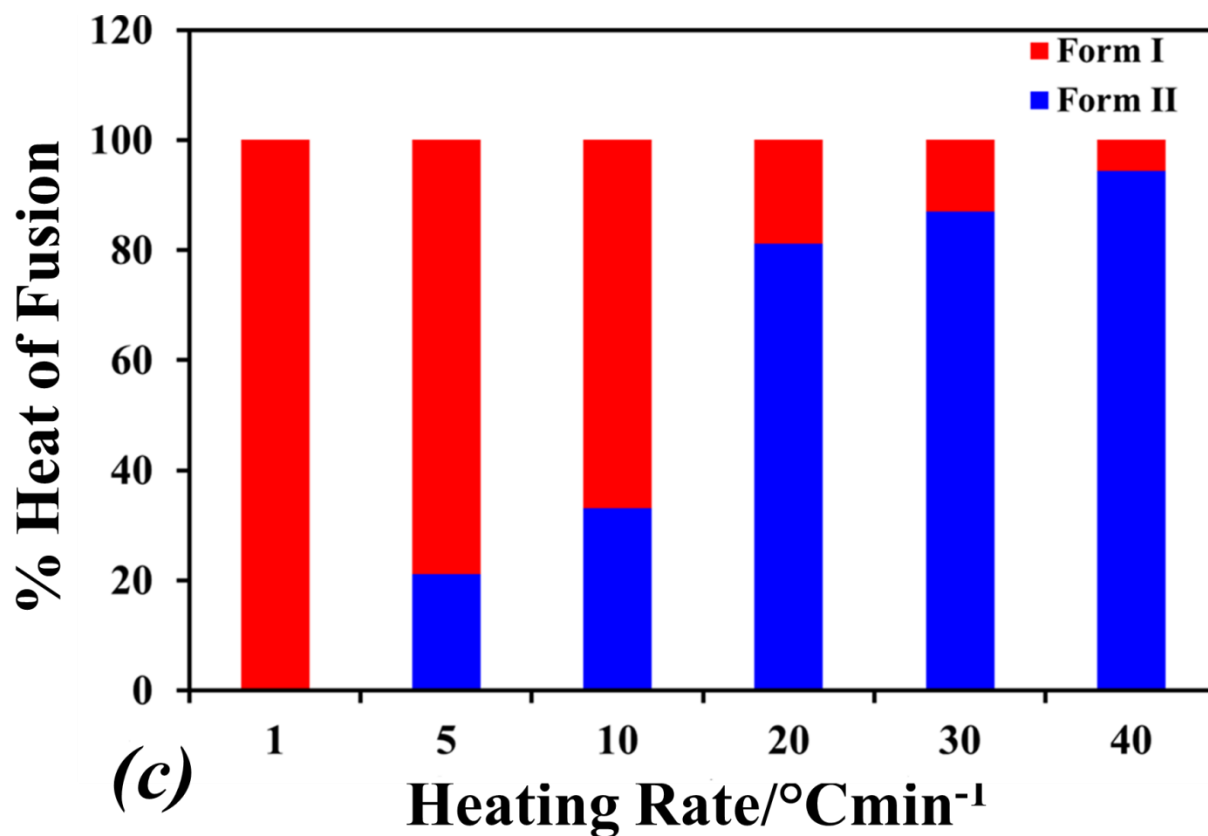
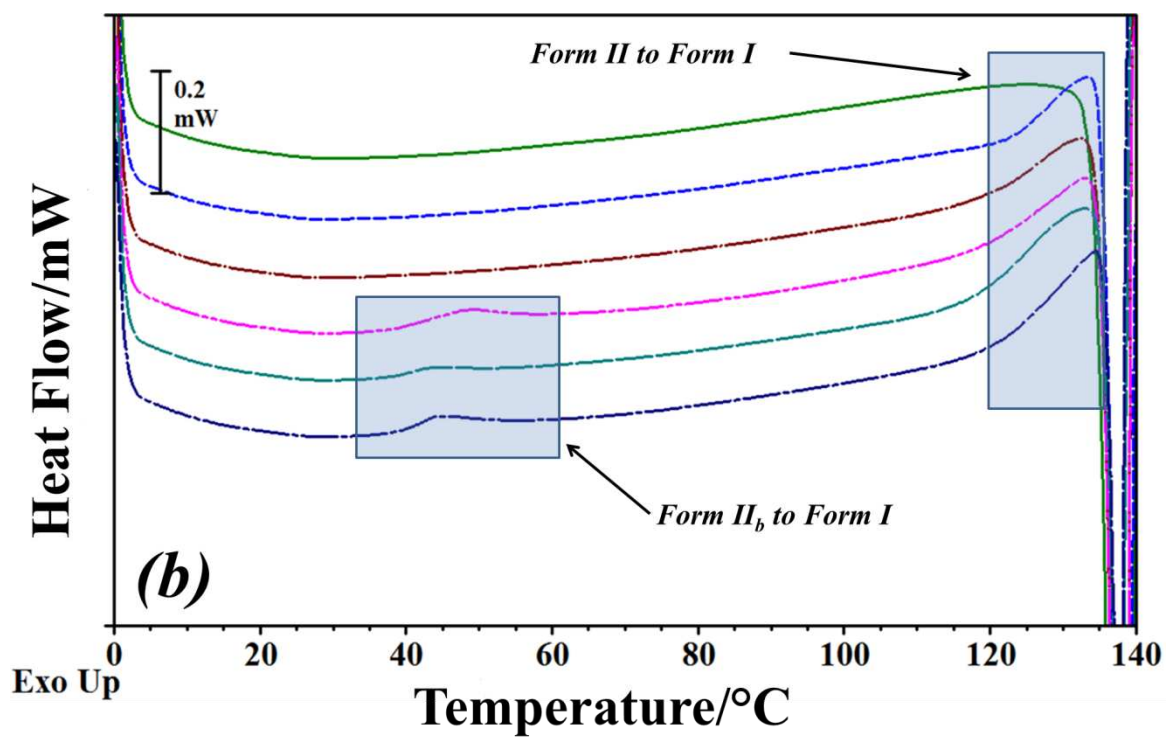
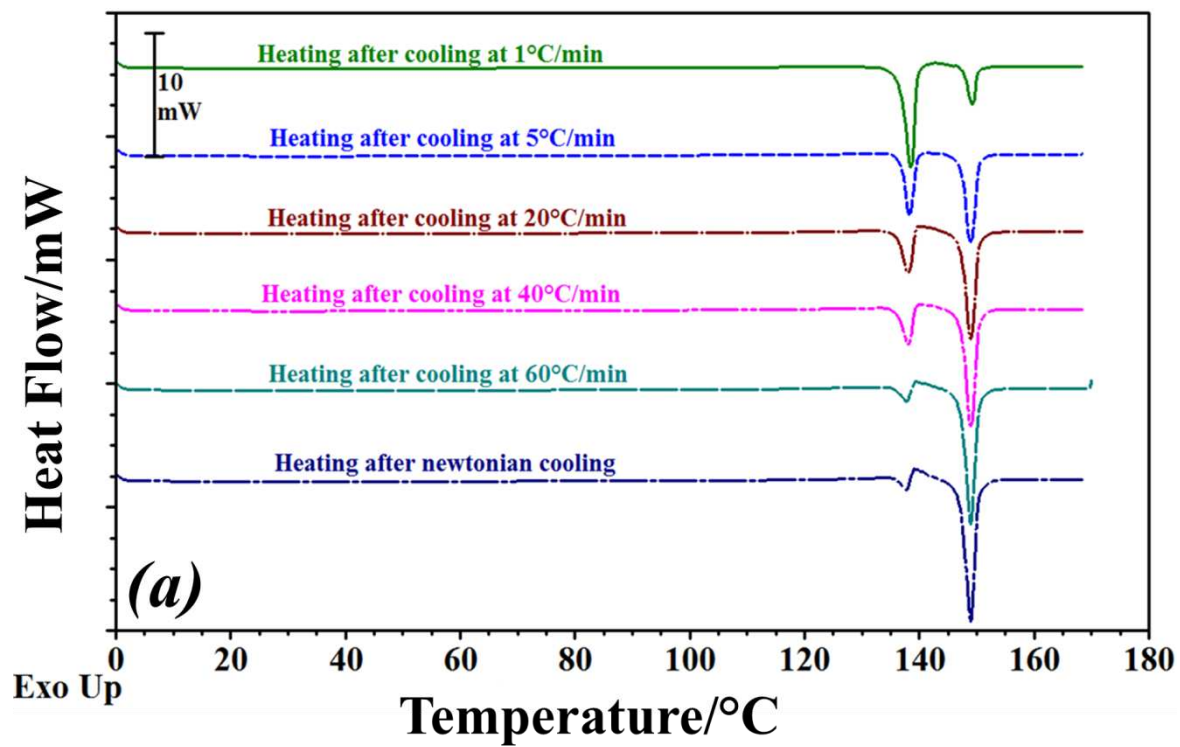
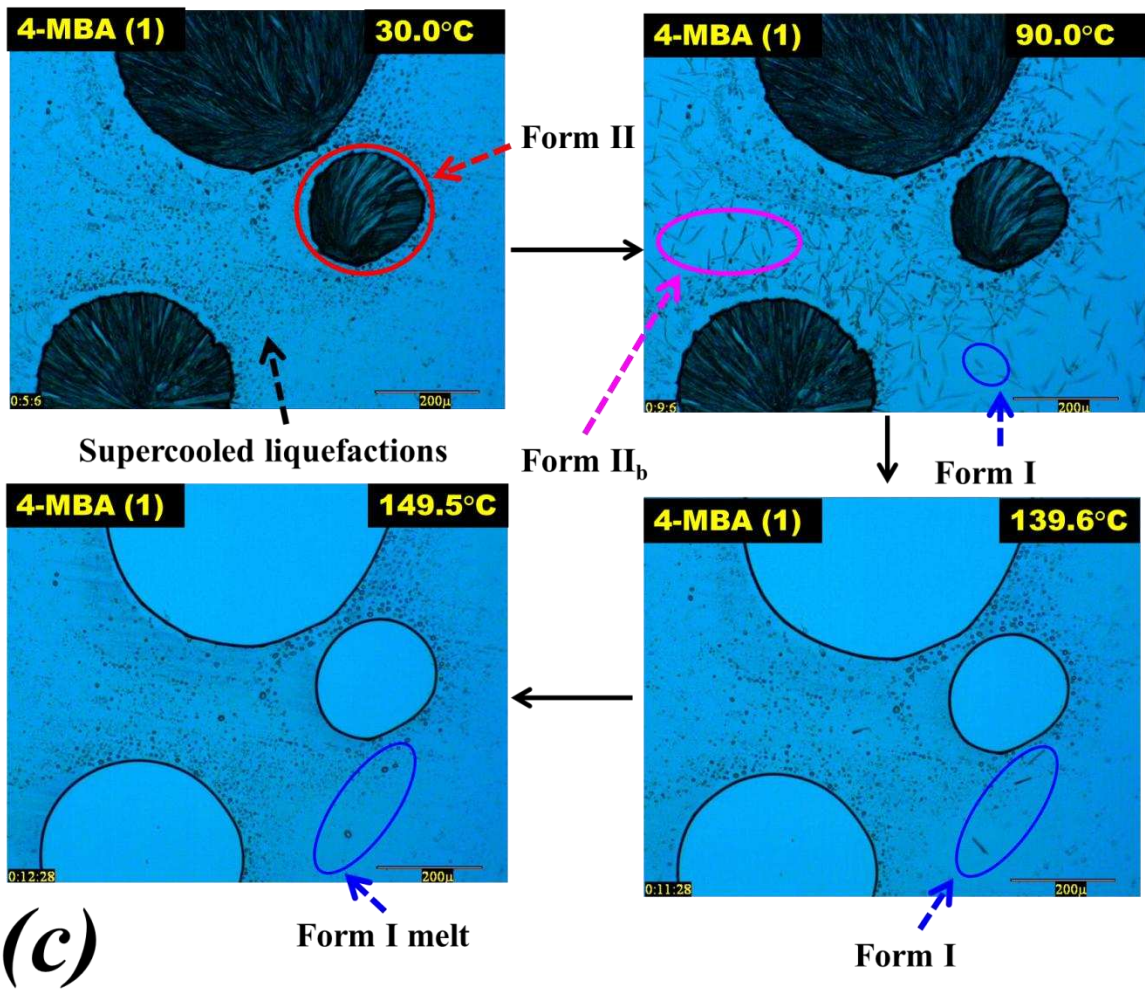


Fig. 7. (a) DSC curve of 4-MBA (1) at different heating rates (1 to $40^{\circ}\text{Cmin}^{-1}$) after cooling at $10^{\circ}\text{Cmin}^{-1}$, (b) expanded area of the DSC curve obtained at $1^{\circ}\text{Cmin}^{-1}$ heating rate and (c) the fractional contribution of the heat of fusion of Form II and Form I to the total heat of fusion as a function of heating rate.





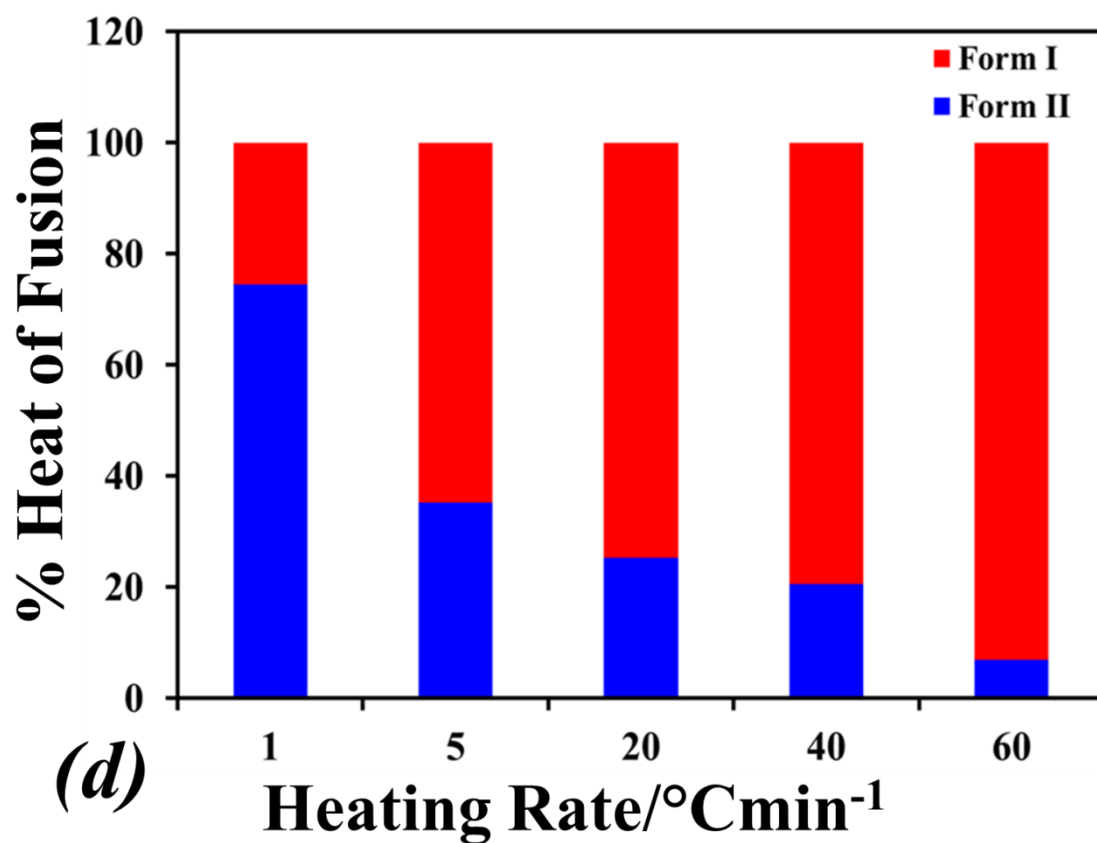
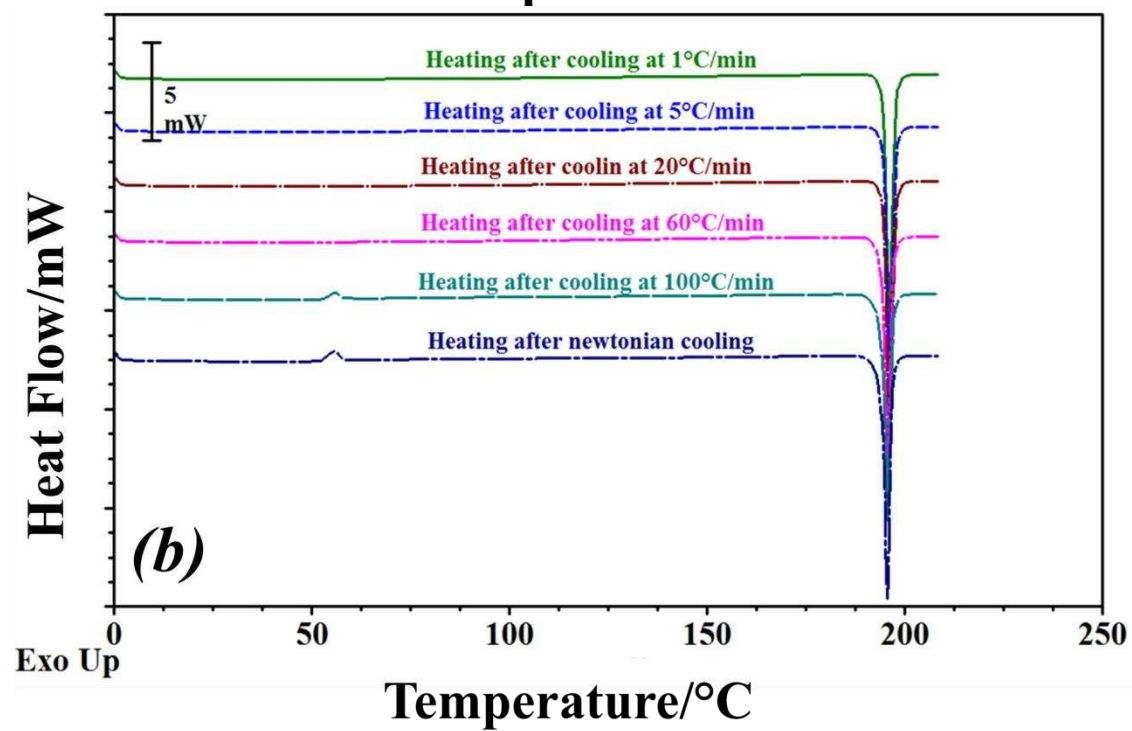
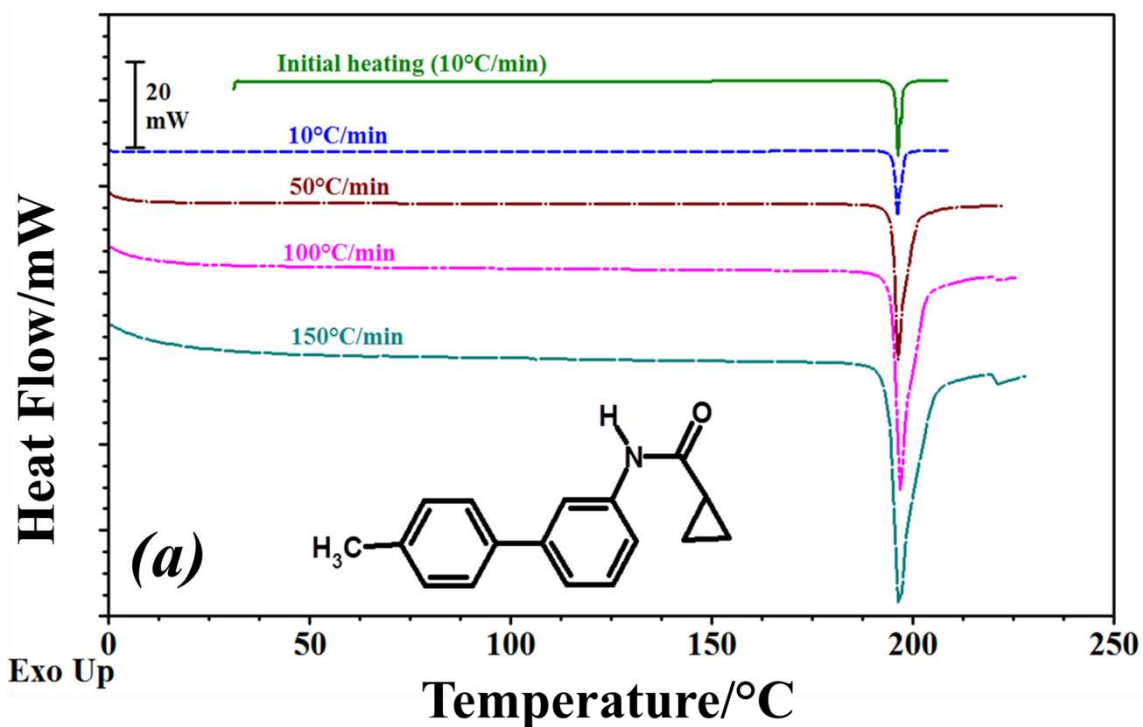


Fig. 8. (a) DSC curve of 4-MBA (1) obtained at a heating rate of 10°Cmin⁻¹ after cooling at various rates (see graph for details), (b) expanded area of the DSC curve obtained at different heating rates, (c) HSM images of key transitions observed for 4-MBA (1) when heated at 10°Cmin⁻¹ between 25 and 170°C after Newtonian cooling of the melt and (d) the fractional contribution of the melting enthalpies of Form II and Form I to the total heat of fusion as a function of cooling rate.



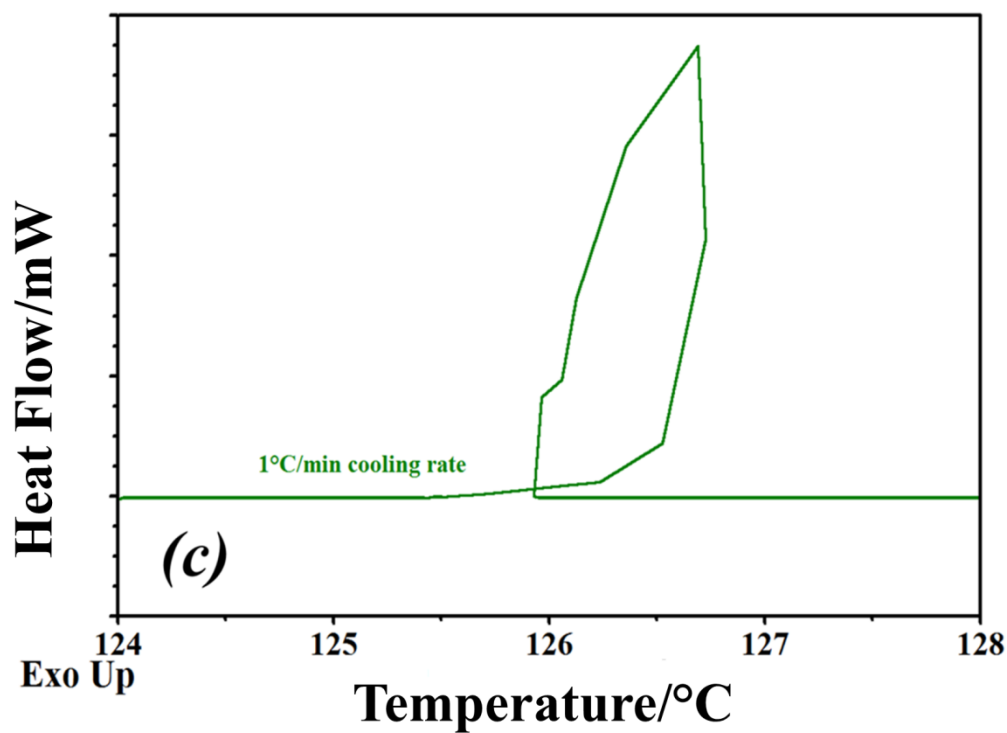
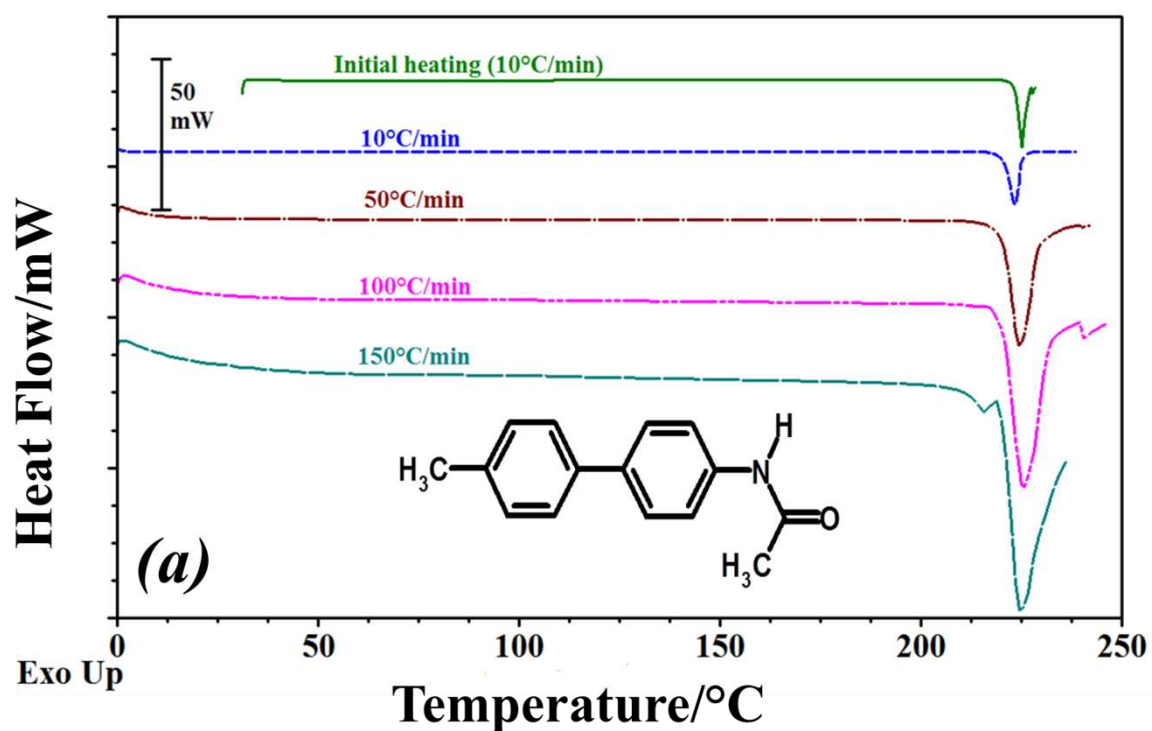


Fig. 9. (a) DSC curves of 4-MBA (2), (a) at various heating rates after cooling at $10^{\circ}\text{Cmin}^{-1}$, (b) at a heating rate of $10^{\circ}\text{Cmin}^{-1}$ after cooling at various cooling rates (see graph for details) and (c) expanded area of the DSC curves obtained at a cooling rate of $1^{\circ}\text{Cmin}^{-1}$.



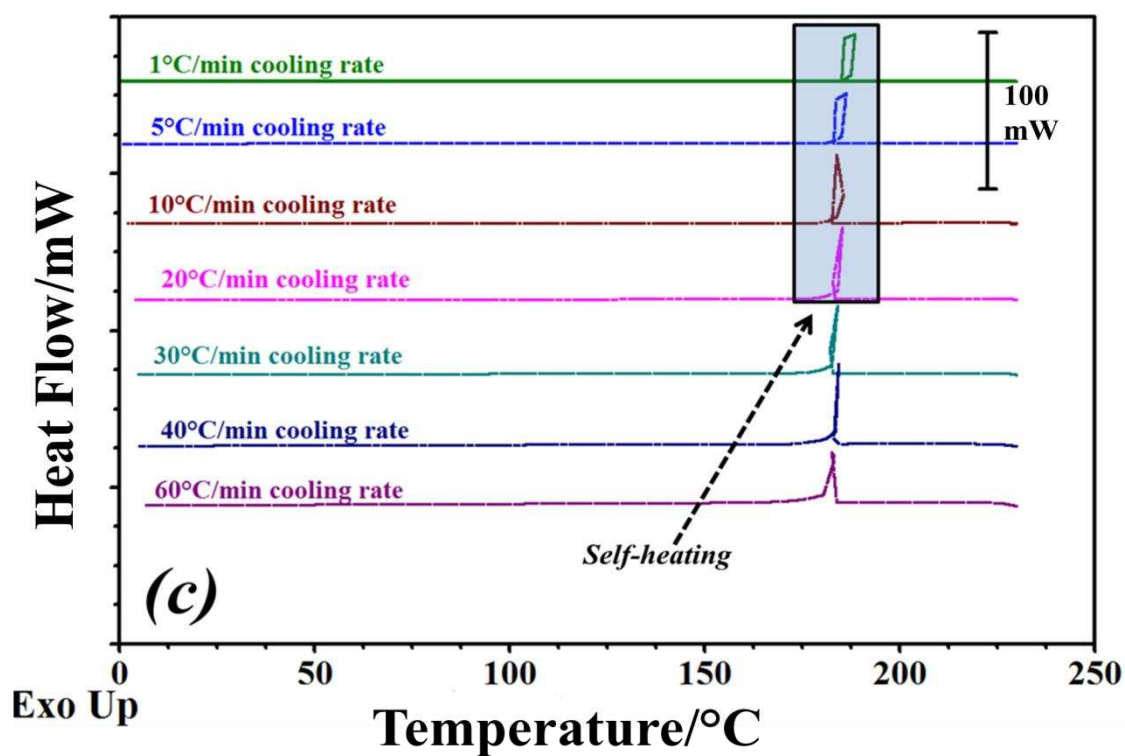
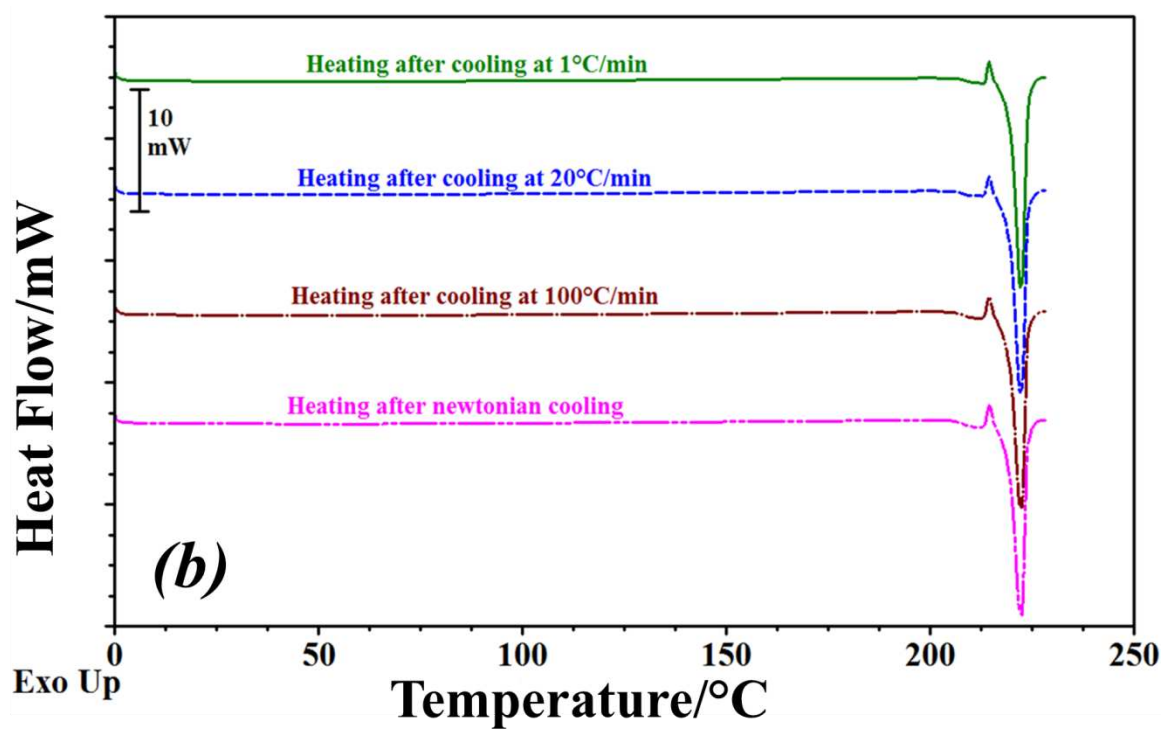
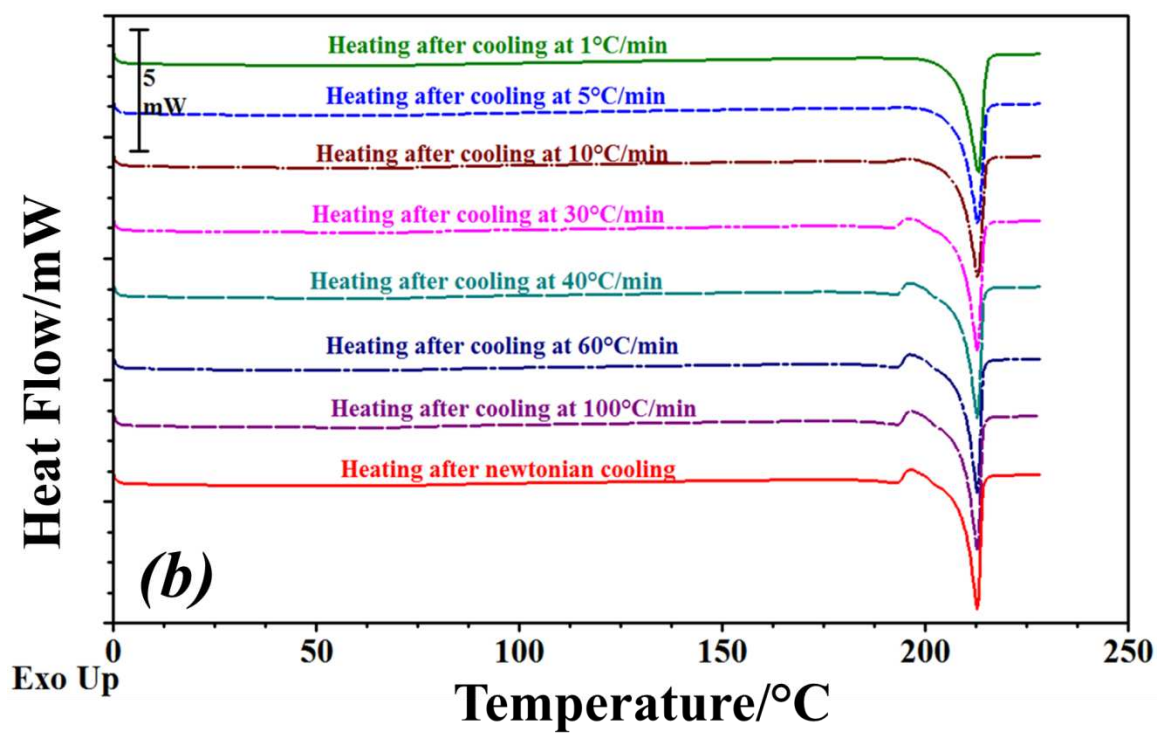
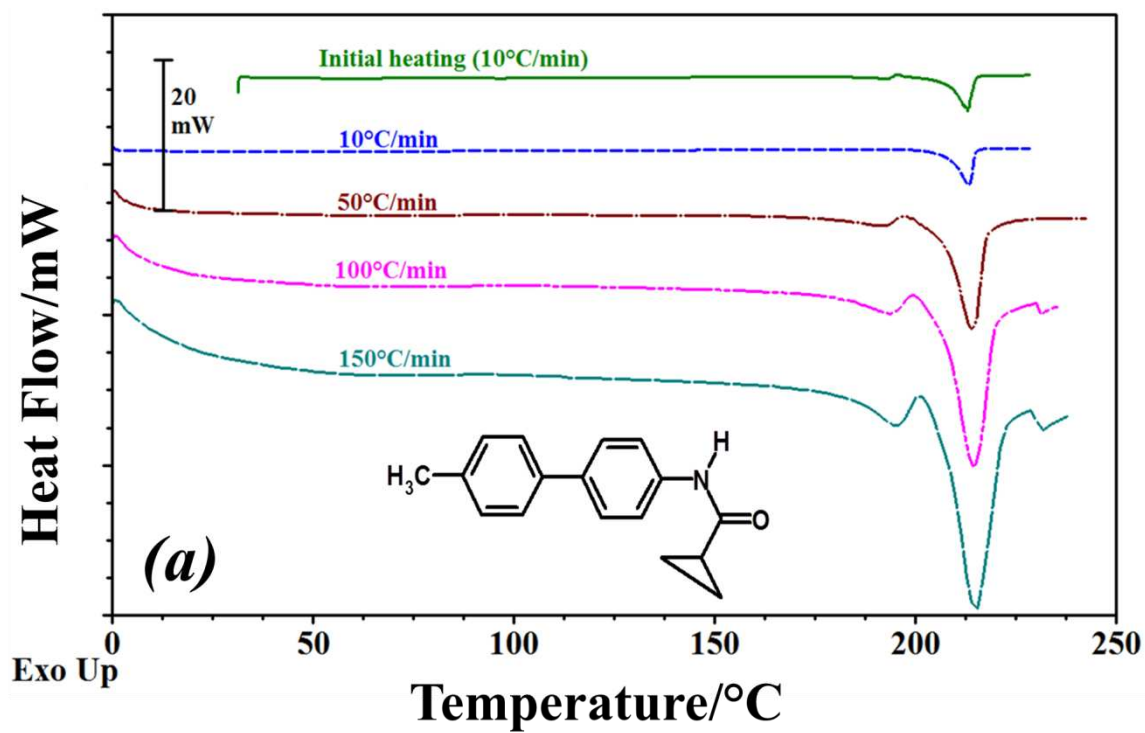


Fig. 10. (a) DSC curves of 4-MBA (3), (a) at various heating rates after cooling at 10°Cmin⁻¹, (b) at a heating rate of 10°Cmin⁻¹ after cooling at various cooling rates and (c) DSC curves obtained at different cooling rates.



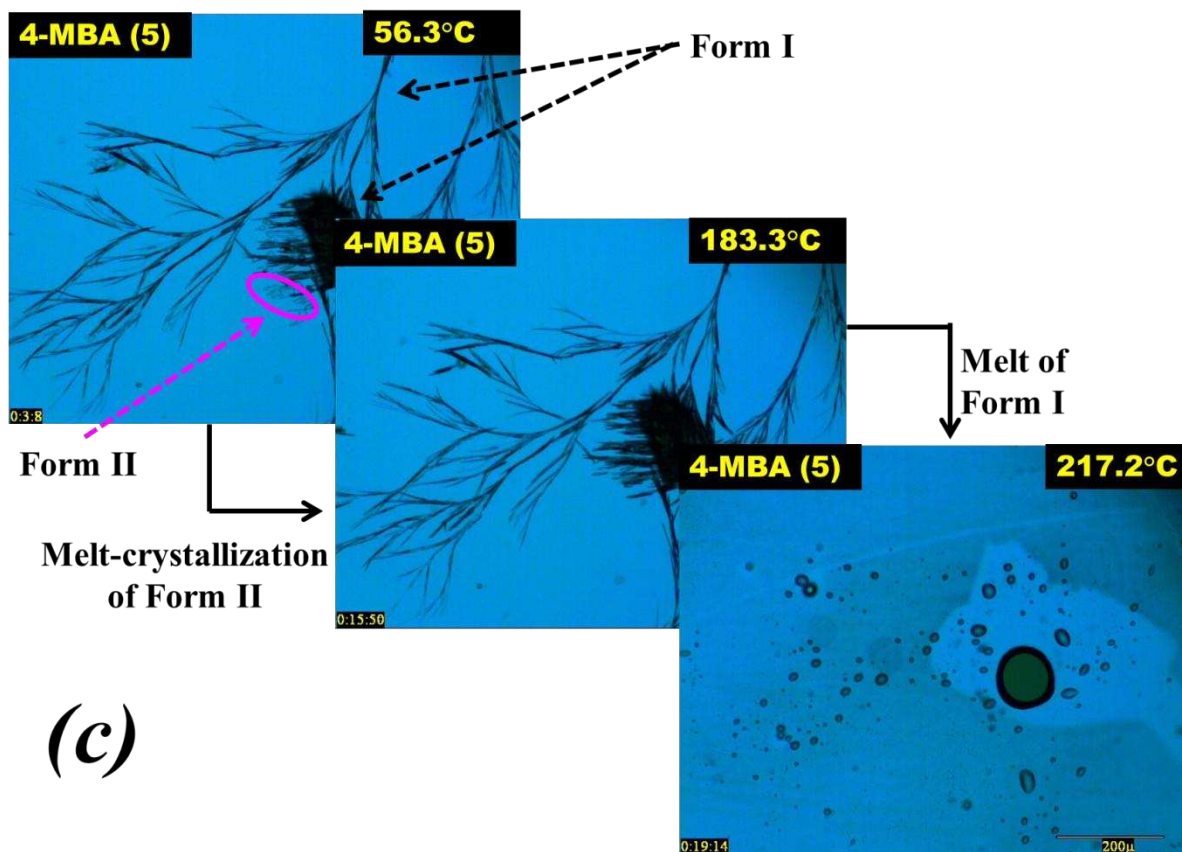


Fig. 11. (a) DSC curves of 4-MBA (5) obtained at different heating rates after cooling at $10^{\circ}\text{Cmin}^{-1}$, (b) at a heating rate of $10^{\circ}\text{Cmin}^{-1}$ after cooling at various cooling rates and (c) HSM images of key transitions observed for 4-MBA (5) when heated at $10^{\circ}\text{Cmin}^{-1}$ between 25 and 250°C after Newtonian cooling of the melt in the HSM.

Table 1. Molecular structures of the 4-methyl-biphenylamide derivatives.

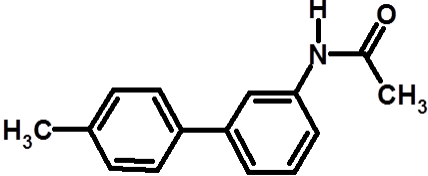
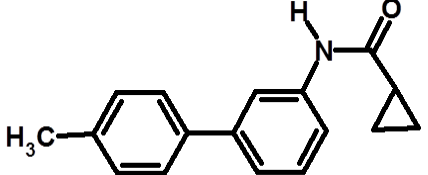
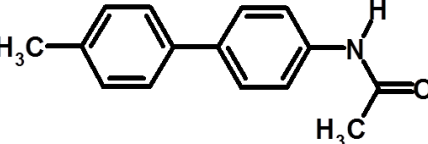
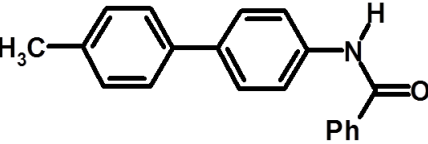
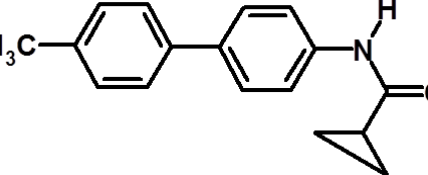
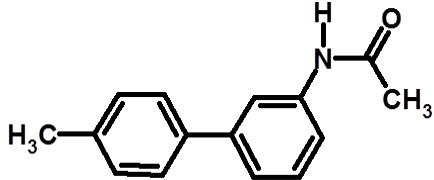
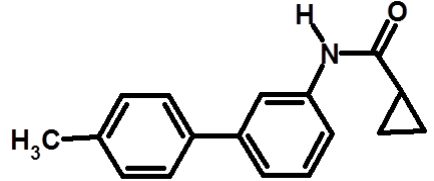
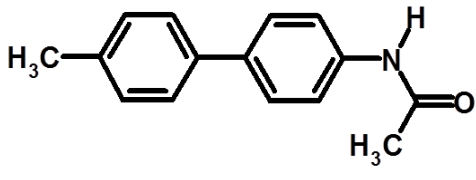
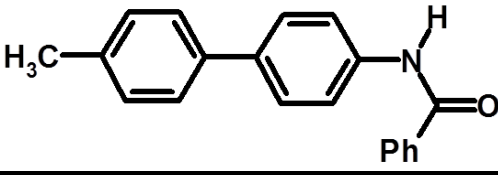
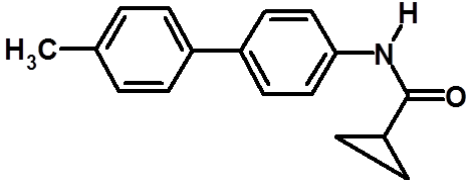
Sample ID	Sample name	Baltus et al, (2012) compound reference	Molecular structure
4-MBA (1)	N-(4'-Methylbiphenyl-3-yl)acetamide	(6i)	
4-MBA (2)	N-(4'-Methylbiphenyl-3-yl) cyclopropanecarboxamide	(6h)	
4-MBA (3)	N-(4'-Methylbiphenyl-4-yl)acetamide	(6b)	
4-MBA (4)	N-(4'-Methylbiphenyl-4-yl)benzamide	(6e)	
4-MBA (5)	N-(4'-Methylbiphenyl-4-yl) cyclopropanecarboxamide	(6a)	

Table 2. Fractional weight changes (ΔW (%)) and peak temperatures for processes detected by TG for the 4-methyl-biphenylamide derivatives.

Sample	1 st process		2 nd Process		Total
	$\Delta W/\%$	Peak temperature/ $^{\circ}\text{C}$	$\Delta W/\%$	Peak temperature/ $^{\circ}\text{C}$	$\Delta W/\%$
4-MBA (1)	100	322 ± 1	-	-	100
4-MBA (2)	100	341 ± 1	-	-	100
4-MBA (3)	100	331 ± 1	-	-	100
4-MBA (4)	100	380 ± 1	-	-	100
4-MBA (5)	2.5 ± 0.3	194 ± 1	98 ± 0.5	347 ± 1	100

Table 3. Apparent activation energies ($n = 2$) obtained for the 4-methyl-biphenylamide derivatives using MTG.

Sample	Structure	E_a (kJmol^{-1})
4-MBA (1)		75 ± 7
4-MBA (2)		78 ± 5
4-MBA (3)		97 ± 12
4-MBA (4)		90 ± 8
4-MBA (5)		99 ± 14